IAI Journals.ASM.org

BB0238, a Presumed Tetratricopeptide Repeat-Containing Protein, Is Required during *Borrelia burgdorferi* Mammalian Infection

Ashley M. Groshong,[a] Danielle E. Fortune,[a] Brendan P. Moore,[a] Horace J. Spencer,[b] Robert A. Skinner,[c] William T. Bellamy,[d] Jon S. Blevins[a]

Departments of Microbiology and Immunology,[a] Biostatistics,[b] Orthopedic Surgery,[c] and Pathology,[d] University of Arkansas for Medical Sciences, Little Rock, Arkansas, USA

The Lyme disease spirochete, *Borrelia burgdorferi*, occupies both a tick vector and mammalian host in nature. Considering the unique enzootic life cycle of *B. burgdorferi*, it is not surprising that a large proportion of its genome is composed of hypothetical proteins not found in other bacterial pathogens. *bb0238* encodes a conserved hypothetical protein of unknown function that is predicted to contain a tetratricopeptide repeat (TPR) domain, a structural motif responsible for mediating protein-protein interactions. To evaluate the role of *bb0238* during mammalian infection, a *bb0238*-deficient mutant was constructed. The *bb0238* mutant was attenuated in mice infected via needle inoculation, and complementation of *bb0238* expression restored infectivity to wild-type levels. *bb0238* expression does not change in response to varying culture conditions, and thus, it appears to be constitutively expressed under *in vitro* conditions. *bb0238* is expressed in murine tissues during infection, though there was no significant change in expression levels among different tissue types. Localization studies indicate that BB0238 is associated with the inner membrane of the spirochete and is therefore unlikely to promote interaction with host ligands during infection. *B. burgdorferi* clones containing point mutations in conserved residues of the putative TPR motif of BB0238 demonstrated attenuation in mice that was comparable to that in the *bb0238* deletion mutant, suggesting that BB0238 may contain a functional TPR domain.

Borrelia burgdorferi, the causative agent of Lyme disease, is a zoonotic pathogen that utilizes an arthropod vector (i.e., *Ixodes* sp. hard ticks) for transmission between a vertebrate reservoir and humans (1–3). As the tick feeds, bacteria are introduced into a mammalian host to establish an initial localized infection at the bite site, after which the bacteria disseminate throughout the mammal and colonize other secondary tissues, such as the heart, joints, and central nervous system (4, 5). *B. burgdorferi* induces disease in the mammalian host, primarily due to its highly invasive nature and its ability to persist in various tissues. Therefore, *B. burgdorferi* virulence factors can be broadly defined as being encoded by genes that contribute to successful arthropod colonization, vector-mediated transmission, or vertebrate infection.

Considering the specialized enzootic life cycle of *B. burgdorferi*, it is not surprising that the *B. burgdorferi* genome contains many genes that are unique among bacterial pathogens (6). These hypothetical proteins are particularly interesting because they represent a group of borrelial proteins that might contribute to vector and/or mammalian colonization and, ultimately, may provide insight into molecular mechanisms contributing to host/vector-pathogen interactions. Although studying genes with unknown functions represents a challenge, a number of these unique *B. burgdorferi* proteins (i.e., BptA, BB0323, BBA52, BBA57, BBA62, and BBA64) are now known to play roles at different stages of the spirochete's enzootic cycle (7–12). Elucidation of the roles of individual hypothetical proteins in *B. burgdorferi* and identification of those necessary for mammalian infection would potentially provide new avenues of intervention or therapeutic targets.

BB0238 is a chromosomally encoded hypothetical protein unique to *B. burgdorferi* that is predicted to be 30 kDa in size and to contain a tetratricopeptide repeat (TPR) domain (6, 13). To evaluate the role of *bb0238* during mammalian infection, a *bb0238*-deficient mutant of *B. burgdorferi* was generated. The *bb0238* mutant was significantly attenuated in the murine borreliosis infection model. Specifically, spirochetes could not be cultured from ear punch or heart tissues recovered from any of the mice infected with the *bb0238* mutant. The *bb0238* mutant also exhibited a defect in its capacity to infect tibiotarsal and bladder tissues. Interestingly, multiple clones expressing *bb0238* with individual point mutations engineered in the putative TPR domain exhibited attenuated infectivity similar to that observed with the *bb0238* deletion mutant, thus suggesting that this domain may be essential to the function of BB0238 in the spirochete. However, it is not likely that BB0238 directly interacts with host cells and/or ligands, because BB0238 partitioned to the inner membrane of *B. burgdorferi* during cellular localization assays. While we were unable to determine the exact function of BB0238, these studies did identify a new protein that plays an important role during *B. burgdorferi* murine infection.

MATERIALS AND METHODS

Bacterial strains and culture conditions. The strains and plasmids utilized in this study are described in Table 1. *Escherichia coli* strains TOP10F′ (Life Technologies, Carlsbad, CA) and MON1 (Monserate, San Diego, CA) were used for plasmid propagation and cloning. *E. coli*

Received 25 April 2014 Returned for modification 29 May 2014
Accepted 23 July 2014
Published ahead of print 28 July 2014
Editor: A. Camilli
Address correspondence to Jon S. Blevins, jsblevins@uams.edu.
Supplemental material for this article may be found at http://dx.doi.org/10.1128/IAI.01977-14.

doi:10.1128/IAI.01977-14

TABLE 1 Plasmids and strains used in this study

Plasmid or strain	Description[a]	Source
Plasmids		
pGEM-T Easy	TA cloning vector; Amp^r	Promega
pJSB430A	pGEM-T Easy-*bb0238*::P*flgB*-Kan mutation construct; Kan^r	This study
pJSB201	pJD7 with the NdeI site in P*flgB-aadA* mutated; $Spec^r$ $Strep^r$	This study
pJD7	Borrelial shuttle vector derived from pKFSS1	18
pJSB445	pJSB201::*bb0238* ORF complementation vector; $Spec^r$ $Strep^r$	This study
pProEX-HTb	Expression construct; N-terminal, TEV-cleavable His_6 tag; Amp^r	Life Technologies
pJSB482	pProEX-HTb::codon-adapted *bb0238* ORF; no signal peptide; Amp^r	This study
pJSB568	pGEM-T Easy::*flaB-actin* qPCR standard; Amp^r	This study
pJSB641	pGEM-T Easy::*flaB* probe; Amp^r	This study
pJSB643	pGEM-T Easy::*bb0238* probe; Amp^r	This study
piRrp2(Kan)	Borrelial shuttle vector with IPTG-inducible *rrp2*; Kan^r	17
pJSB499	piRrp2(Kan) with *rrp2* replaced by the *ebfC* ORF; Kan^r	This study
pJSB598	pJSB445 with $BB0238_{Y43A}$ mutation; $Spec^r$ $Strep^r$	This study
pJSB599	pJSB445 with $BB0238_{G47V}$ mutation; $Spec^r$ $Strep^r$	This study
pJSB603	pJSB445 with $BB0238_{Y50A}$ mutation; $Spec^r$ $Strep^r$	This study
pJSB604	pJSB445 with $BB0238_{A66G}$ mutation; $Spec^r$ $Strep^r$	This study
pJSB602	pJSB445 with $BB0238_{P71A}$ mutation; $Spec^r$ $Strep^r$	This study
Strains		
E. coli		
TOP10F′	F′ [*lacI*^{q}Tn*10*(Tet^r)] *mcrA* Δ(*mrr-hsdRMS-mcrBC*) ϕ80*lacZ*ΔM15 *nupG* Δ*lacX74 recA1 ara*Δ*139* Δ(*ara-leu*)*7697 galU galK rpsL* (Str^r) *endA1*	Life Technologies
MON1	F^- *endA1 recA1 mcrA* Δ(*mrr-hsdRMS-mcrBC*) ϕ80*lacZ*ΔM15Δ*lacX74 ara*Δ*139* Δ(*ara-leu*)*7697 galU galK nupG rpsL* λ^-	Monserate
C41(DE3)	F^- ompT hsdSB (r_B^- m_B^-) gal dcm (DE3)	Lucigen
B. burgdorferi		
Bb297	Strain 297; infectious human spinal fluid isolate	14
BbΔ*bb0238*	Bb297 with *bb0238* interrupted with P*flgB*-Kan marker; Kan^r	This study
Bb*bb0238*^{C}	BbΔ*bb0238* complemented with pJSB445; Kan^r $Strep^r$	This study
BbiEbfC	Bb297 transformed with pJSB499; Kan^r	This study
Bb*bb0238*$_{Y43A}$	BbΔ*bb0238* complemented with pJSB598; Kan^r $Strep^r$	This study
Bb*bb0238*$_{G47V}$	BbΔ*bb0238* complemented with pJSB599; Kan^r $Strep^r$	This study
Bb*bb0238*$_{Y50A}$	BbΔ*bb0238* complemented with pJSB603; Kan^r $Strep^r$	This study
Bb*bb0238*$_{A66G}$	BbΔ*bb0238* complemented with pJSB604; Kan^r $Strep^r$	This study
Bb*bb0238*$_{P71A}$	BbΔ*bb0238* complemented with pJSB602; Kan^r $Strep^r$	This study

[a] Spec, spectinomycin; Strep, streptomycin; Amp, ampicillin; Kan, kanamycin.

C41(DE3) (Lucigen, Middleton, WI) was used for expression of recombinant protein for purification. *E. coli* transformants were selected in Luria-Bertani medium supplemented with 100 μg/ml of ampicillin, 100 μg/ml of spectinomycin, or 50 μg/ml of kanamycin (Kan). The low-passage human isolate *B. burgdorferi* strain 297 (Bb297) was used in these studies (14). Unless noted, *B. burgdorferi* was grown in Barbour-Stoenner-Kelley-II (BSK-II) medium at 37°C with 3% CO_2 and antibiotics when appropriate (150 μg/ml streptomycin [Strep] or 150 μg/ml kanamycin) (15). Transformation of *B. burgdorferi* was carried out as previously described (16).

Generation and confirmation of plasmids and clones used in this study. The primers used in this study are summarized in Table S1 in the supplemental material. When PCR amplifying fragments for cloning, genomic DNA (gDNA) from Bb297 served as the template, and TaKaRa PrimeStar HS DNA Polymerase (Clontech, Mountain View, CA) was used for amplification. The amplicons were TA cloned into pGEM-T Easy (Promega Corp., Madison, WI) and confirmed by sequencing. Fermentas GeneRuler DNA ladder mix was the molecular weight standard used for DNA electrophoresis (Thermo Scientific, Rockford, IL). The endogenous plasmid content of each transformant was confirmed by PCR-based plasmid profiling (16).

The *bb0238* mutant, BbΔ*bb0238*, was created by first amplifying regions flanking *bb0238* (accession no. NP_212372) with primers that introduced an AscI restriction site on the 3′ end of a 1,009-bp upstream flanking region (5′ F1-BB0238 and 3′ F1-BB0238-AscI) (see Table S1 in the supplemental material) and a 5′ AscI and a 3′ BssHII site in a 995-bp downstream flanking region (5′ F2-BB0238-AscI and 3′ F2-BB0238-BssHII) (see Table S1 in the supplemental material). To ligate the two flanking regions, the downstream F2 fragment was excised using BssHII and ligated into the vector containing the upstream F1 region linearized with AscI. A Kan^r marker with a T7 transcriptional terminator fused to the end of the resistance gene, designated *flgBp-aphI*-T7t, was provided by Scott Samuels at the University of Montana (17). The Kan^r marker was ligated into the unique AscI restriction site at the junction between the two flanking regions. The final mutagenesis construct, designated pJSB430A, contained a Kan^r marker that replaced an internal region of the *bb0238* open reading frame (ORF) between bp 259 and 500. The pJSB430A mutagenesis construct was electroporated into Bb297, and transformants were selected with kanamycin. Interruption of *bb0238* in the chromosome by the Kan^r marker was confirmed with *bb0238* diagnostic primers (5′ BB0238-Diag and 3′ BB0238-Diag) (see Table S1 in the supplemental material).

To restore *bb0238* expression in the BbΔ*bb0238* mutant, the *bb0238* ORF, along with 420 bp upstream and 258 bp downstream of the ORF, was amplified using primers that introduced BamHI restriction sites on the 5′ and 3′ ends (5′ BB0238-Comp and 3′ BB0238-Comp) (see Table S1 in the supplemental material). This region was ligated into pJSB201, a derivative of the cp9-based pJD7 shuttle vector (18). The insert was con-

firmed by sequencing with vector-specific primers and internal primers, 5′ BB0238-Int and 3′ BB0238-Int (see Table S1 in the supplemental material). The resulting construct, designated pJSB445, contained the *bb0238* ORF, along with a region containing its putative native promoter and a P*flgB-aadA* Strep^r resistance marker. pJSB445 was electroporated into BbΔ*bb0238* with kanamycin selection during recovery and plated with kanamycin and streptomycin selection. The presence of pJSB445 in transformants was confirmed by plasmid recovery and PCR using *bb0238* diagnostic primers (5′ BB0238-Diag and 3′ BB0238-Diag) (see Table S1 in the supplemental material). BbΔ*bb0238* transformed with pJSB445 was designated Bb*bb0238*^{C}.

To produce recombinant BB0238 protein, the *bb0238* ORF from Bb297 was first codon adapted to optimize expression in *E. coli* using GeneArt gene synthesis (Life Technologies). The codon-optimized ORF was PCR amplified using primers that introduced BamHI and EcoRI restriction sites on the 5′ and 3′ ends, respectively (5′ BB0238 Opt-SP/BamHI and 3′ BB0238 Opt/EcoRI) (see Table S1 in the supplemental material). These primers were designed to exclude the N-terminal 26 amino acids of BB0238, which was predicted by SignalP 4.1 to contain either a signal peptidase I cleavage site or a transmembrane domain (19). The ORF fragment was confirmed by sequencing and ligated into the pPROEX-HTb expression vector (Life Technologies) to generate pJSB482.

To generate copy number standards for quantitative PCR (qPCR) analysis of bacterial burdens in tissues, a region of the murine β-actin gene was amplified from C3H/HeN DNA using primers ActF-STD and ActR-STD (see Table S1 in the supplemental material) (20), which introduced a BamHI restriction site at one end. The amplicon was cloned into pGEM-T Easy. A region of *flaB* was then amplified from Bb297 gDNA using primers *flaB*F-STD and *flaB*R-STD (see Table S1 in the supplemental material). These primers introduced BamHI restriction sites on both ends of the fragment. The *flaB* amplicon was cloned into pGEM-T Easy containing the actin fragment using BamHI restriction enzyme sites. The resulting construct was designated pJSB568.

To generate hybridization probes for Northern blot analyses, regions corresponding to the genes of interest were amplified and cloned into pGEM-T Easy. The primers 5′ BB0238-probe and 3′ BB0238-probe amplified the DNA fragment probe for *bb0238* (see Table S1 in the supplemental material). The primers for *flaB* (*flaB*d and *flaB*rc) (see Table S1 in the supplemental material) were based on those used by Bugrysheva et al. (21). The vectors were designated pJSB641 and pJSB643 for the *flaB* and *bb0238* Northern hybridization probes, respectively.

To generate the *B. burgdorferi* clone expressing IPTG (isopropyl-β-D-thiogalactopyranoside)-inducible *ebfC*, the *ebfC* ORF was amplified with primers that introduced NdeI and HindIII restriction enzyme sites at the 5′ and 3′ ends, respectively (5′ EbfC-NdeI and 3′ EbfC-HindIII) (see Table S1 in the supplemental material). The *rrp2* ORF in piRrp2(Kan) (17) was then replaced by the *ebfC* ORF to generate pJSB499. pJSB499 was transformed into Bb297, and Kan^r transformants were recovered. The presence of pJSB499 in clones was confirmed by plasmid recovery in *E. coli*. A single clone, designated BbiEbfC, was selected for characterization.

To generate *B. burgdorferi* clones expressing *bb0238* with point mutations in the putative TPR domain, overlap extension PCR was used to mutate individual amino acids encoded in the *bb0238* ORF of the complementation construct, pJSB445. Primers 5′ BB0238-Comp and 3′ BB0238-Comp (see Table S1 in the supplemental material) represent the outermost primers used for all amplifications. Internal primers used to mutate individual residues (i.e., Y43A, G47V, Y50A, A66G, and P71A) are indicated with their respective mutation denoted as sense or antisense in Table S1 in the supplemental material. Primers 5′ BB0238-Comp and 3′ BB0238-Comp were paired with the mutational sense and antisense primers, respectively. Amplicons from the individual reactions were gel purified and combined to serve as DNA templates in a second round of amplification using the outermost 5′ BB0238-Comp and 3′ BB0238-Comp primers. The mutated *bb0238* alleles were ligated into pJSB201 to produce pJSB598 (*bb0238*$_{Y43A}$), pJSB599 (*bb0238*$_{G47V}$), pJSB603 (*bb0238*$_{Y50A}$), pJSB604 (*bb0238*$_{A66G}$), and pJSB602 (*bb0238*$_{P71A}$). The inserts were confirmed by sequencing with vector-specific primers and internal primers, 5′ BB0238-Int and 3′ BB0238-Int. BbΔ*bb0238* was transformed with each plasmid, and single clones were recovered for genotyping. The presence of the shuttle vector in the transformants was confirmed by PCR using *bb0238* diagnostic primers (5′ BB0238-Diag and 3′ BB0238-Diag) (see Table S1 in the supplemental material), as well as plasmid recovery from *E. coli* and sequencing. Confirmed clones were designated according to the BB0238 mutation that each transformant carried: Bb*bb0238*$_{Y43A}$, Bb*bb0238*$_{G47V}$, Bb*bb0238*$_{Y50A}$, Bb*bb0238*$_{A66G}$, or Bb*bb0238*$_{P71A}$.

Expression and purification of recombinant BB0238 protein. Expression from pProEX-HTb generates a recombinant protein with an N-terminal His$_6$ tag followed by a tobacco etch virus (TEV) protease cleavage site. To produce recombinant BB0238, pJSB482 was transformed into *E. coli* C41(DE3), and cultures were induced for 3 h with 0.5 mM IPTG. The recombinant protein was affinity purified by the batch method with HisPur Ni-nitrilotriacetic acid (NTA) resin (Thermo Scientific) under nonnative conditions according to the manufacturer's instructions, except 8 M urea was used to solubilize the inclusion body pellet and included in all purification buffers. The concentration of purified recombinant BB0238 was determined using the DC protein assay kit (Bio-Rad Laboratories, Hercules, CA).

Generation of BB0238-specific antisera. To generate polyclonal antisera, 25 μg of recombinant protein in 200 μl of sterile phosphate-buffered saline (PBS) was combined with complete Freund's adjuvant (Sigma, St. Louis, MO) at a 1:1 ratio. After emulsification of the antigen-adjuvant mixture, 3- to 4-week-old female Sprague-Dawley rats (Harlan, Indianapolis, IN) were injected intraperitoneally. The rats were then boosted twice with 25 μg of recombinant protein, mixed, and emulsified as described above with incomplete Freund's adjuvant (Sigma) at 4-week intervals. Sera were collected 2 weeks following the final immunization. The University of Arkansas for Medical Sciences (UAMS) is accredited by the International Association for Assessment and Accreditation of Laboratory Animals Care (AAALAC), and all immunization protocols were approved by the UAMS Institutional Animal Care and Use Committee (IACUC).

SDS-PAGE and immunoblotting. Sodium dodecyl sulfate-polyacrylamide gel electrophoresis (SDS-PAGE) and immunoblot analyses were performed as previously described (16). A volume of cell lysate equivalent to 2×10^7 bacteria was loaded in each gel lane of an SDS-12.5% PAGE gel and separated by electrophoresis. The electrophoresed proteins were either stained with Sypro Ruby stain (Bio-Rad) or transferred to nitrocellulose membranes for colorimetric immunoblot detection, using 4-chloro-1-naphthol as the substrate. For chemiluminescence detection with SuperSignal West Dura Extended Duration Substrate (Thermo Scientific), proteins were transferred to polyvinylidene difluoride (PVDF) membranes. Antibodies and antisera used for detection of FlaB, BB0796, OspA, DbpA, and OspC were previously described (16, 22, 23). BB0238-specific antiserum production is described above. The molecular mass standard used for all immunoblots was the All Blue Precision Plus marker (Bio-Rad). Bio-Rad Low Range Unstained SDS-PAGE standards were used for Sypro Ruby-stained SDS-PAGE gels.

Infection of mice by needle inoculation. All murine infection experiments were approved by the UAMS institutional IACUC. Four- to 5-week-old C3H/HeN mice (Harlan) were used for mouse infection studies. Four- to 5-week-old CBYSmn.CB17-*Prkdc*^{scid}/J mice (Jackson Laboratories, Bar Harbor, ME) were used for immunocompromised *scid* mouse infection studies. Clones were grown to the mid-log phase with antibiotic selection, at which time the bacterial density in each culture was enumerated using dark-field microscopy and diluted appropriately. Mice were infected via intradermal injection in the sternal region of the thorax as previously described (16). To determine the 50% infectious dose (ID_{50}) for Bb297, BbΔ*bb0238*, and Bb*bb0238*^{C}, mice were injected with serial 10-fold dilutions containing 10^2 to 10^5 bacteria. For all other infection studies, a dose of 10^5 bacteria was used. At 2 weeks postinfection, tissue

samples (i.e., ear punch, back skin, brachial and inguinal lymph nodes, heart, tibiotarsal tissue, and bladder) were harvested and cultured in BSK-II medium supplemented with *Borrelia* antibiotic mixture (BAM) (Monserate). Additional heart, tibiotarsal, and back skin samples were harvested and frozen for qPCR and quantitative real-time PCR (qRT-PCR) analysis (see below). Heart and knee tissues were also collected for histopathology (see below). Cultures containing tissue samples were examined by dark-field microscopy for the presence of spirochetes 1 to 2 weeks after collection. Aliquots of cultures with positive growth were passed to BSK-II supplemented with BAM and confirmed to contain the respective genotype of the isolated bacteria.

Histological assessment. Heart and knee tissues were fixed in 10% neutral buffered formalin, paraffin embedded, routinely processed, and stained with hematoxylin and eosin (H&E). Knees were decalcified in 5% formic acid prior to processing. A blind histological assessment was then performed on stained tissue sections to evaluate the presence and severity of carditis and arthritis in each mouse (24). Sagittal sections through the heart, which included the aorta, were scored for severity of inflammation (0 [absent] to 4 [marked]), aortic involvement (0 [present] or 1 [absent]), pericardial inflammation (0 [present] or 1 [absent]), and endocardial inflammation (0 [present] or 1 [absent]). Sagittal sections through the knee were scored for severity of inflammation (0 [absent] to 4 [marked]), synovial proliferation (0 [present] or 1 [absent]), significance of sheath thickening (0 [absent] to 4 [marked]), and significance of involvement of adjacent tissues (0 [absent] to 4 [marked]). Individual criterion scores were then totaled for a maximum cumulative score of 7 or 13 for carditis and arthritis, respectively.

qPCR analyses of spirochete tissue burden. DNA was extracted from back skin, heart, and tibiotarsal samples from infected mice as previously described by Maruskova et al. (20). DNA was extracted using a High Pure PCR template preparation kit (Roche Applied Sciences, Indianapolis, IN) according to the manufacturer's instructions, except that 200 μg of collagenase (5 mg/ml stock; Sigma) was added during lysis. Purified DNA was analyzed via qPCR on a StepOnePlus Real Time PCR System using TaqMan Fast Advanced master mix (Life Technologies). The primer set and probe used to detect *flaB* were FlaB-ABI-F, FlaB-ABI-R, and FlaB-ABI-Probe. The primer set and probe used to detect the β-actin gene were Act-ABI-F, Act-ABI-R, and Actin-ABI-Probe. The *flaB* and β-actin probes were labeled on the 5′ end with 6-carboxyfluorescein (FAM) and MAX, respectively (Integrated DNA Technologies, Coralville, IA). To quench the probe fluorophores, probes were also labeled at the 3′ end with Iowa Black FQ and internally quenched with ZEN (Integrated DNA Technologies). The number of *flaB* copies was used to quantify spirochetal burdens based on a copy number standard curve using the pJSB568 *flaB*/β-actin vector as a standard. Bacterial burdens were reported as numbers of *flaB* copies per 10^6 copies of mouse β-actin.

Cultivation of *B. burgdorferi* for *in vitro* analyses. For growth curve analyses, cultures of Bb297, BbΔ*bb0238*, and Bb*bb0238*^{C} were inoculated to an initial density of 1×10^3 bacteria/ml in BSK-II medium containing appropriate antibiotic selection. Beginning at 3 days postinoculation, culture densities were determined daily by enumerating spirochetes using dark-field microscopy; 10 fields were counted per culture, and analyses were performed in duplicate. For room temperature growth curves, samples were inoculated at 1×10^3 bacteria/ml, left at room temperature, and counted once a week. BbiEbfC was grown as described above, except cultures were divided at 4 days postinoculation and 1 mM IPTG was added to one portion of the culture. BbiEbfC cultures were then grown for 48 h posttreatment, and cells were collected for analysis.

Transcriptional analysis of *bb0238*. Total RNA was isolated from *in vitro*-cultivated bacteria or murine tissues using TRIzol reagent (Life Technologies) according to the manufacturer's protocol. RNA was purified and DNase treated using the RNeasy minikit and RNase-free DNase I, respectively (Qiagen Inc., Valencia, CA). The presence of contaminating DNA was tested for amplification using TaKaRa EmeraldAmp GT PCR master mix (Clontech) and primers specific for *flaB*.

For qRT-PCR analyses, purified RNA was converted to cDNA using an iScript cDNA synthesis kit according to the manufacturer's instructions. qRT-PCR analyses were performed with the StepOnePlus Real Time PCR System using TaqMan Fast Advanced master mix (Life Technologies). Control reactions prepared without reverse transcriptase were included in the analysis. The primer set and probe used to detect *flaB* transcripts were FlaB-F, FlaB-R, and FlaB-Probe. The primer set and probe used to detect the *bb0238* transcripts were BB0238-F, BB0238-R, and BB0238-Probe. The primer set and probe used to detect *ospC* transcripts were OspC-F, OspC-R, and OspC-Probe. The probes were labeled at the 5′ and 3′ ends with FAM and Black Hole Quencher-1, respectively (Integrated DNA Technologies).

For quantitation of *ebfC* transcripts, qRT-PCR analyses were performed using Power SYBR green (Life Technologies). The primer set used to detect *ebfC* was EbfC-ABI-F and EbfC-ABI-R, and *flaB* was detected using primers FlaB-ABI-F and FlaB-ABI-R. *flaB* transcripts were used as an internal control to normalize qRT-PCR data, and differential expression was determined using the $2^{-\Delta\Delta CT}$ calculation. Results are expressed relative to *flaB*.

To identify the transcriptional start site (TSS) of *bb0238* in Bb297, 5′ rapid amplification of cDNA ends (RACE) was performed using the 5′ RACE system v2.0 (Life Technologies) according to the manufacturer's directions. *bb0238*-specific primers 5′ RACE-GSP1 and 5′ RACE-GSP2 were used for cDNA synthesis and amplification, respectively (see Table S1 in the supplemental material). Amplified fragments were cloned into pGEM-T Easy, and single clones were sequenced with vector-specific primers to determine the TSS.

Reverse transcription-PCR (RT-PCR) was used to evaluate transcriptional linkage of *bb0238* and *bb0239*. The iScript cDNA Synthesis kit (Bio-Rad) was used to synthesize cDNA from Bb297 RNA via random priming. A control reaction mixture lacking reverse transcriptase was also included. cDNA was used as the template for primer pairs corresponding to the *bb0238* ORF (5′ BB0238-Diag and 3′ BB0238-Diag) and the *bb0238-bb0239* intergenic region (5′ BB0238-link and 3′ BB0238-link) (see Table S1 in the supplemental material). Each PCR with cDNA was accompanied by a positive-control reaction that utilized the same set of primers and Bb297 gDNA. All PCR products were analyzed by electrophoresis on a 0.8% agarose gel stained with ethidium bromide.

The Ambion NorthernMax-Gly kit (Life Technologies) was used for Northern blot analyses; 5 μg of denatured RNA from Bb297 and BbΔ*bb0238* was loaded per lane, electrophoresed, and transferred to an Ambion BrightStar-Plus positively charged nylon membrane (Life Technologies) according to the manufacturer's instructions. To generate Northern hybridization probes, the DNA fragments corresponding to *flaB* and *bb0238* were excised from pJSB641 and pJSB643, respectively, using EcoRI and gel purified. The fragments were labeled with digoxigenin (DIG) via random priming using the DIG High Prime DNA labeling and detection starter kit II (Roche) according to the manufacturer's directions. Hybridization was performed according to the conditions provided in the NorthernMax-Gly kit, and detection was carried out according to the protocol outlined in the DIG High Prime DNA labeling and detection starter kit II. The DIG-labeled RNA Molecular Weight Marker I, 0.3 to 6.9 kb (Roche), was included as a standard on all Northern blots.

Subcellular localization studies. To evaluate localization of BB0238 to the bacterial surface, proteinase K accessibility assays were performed as previously described (25). In brief, 2×10^9 spirochetes were incubated in PBS with 5 mM $MgCl_2$ (PBS-$MgCl_2$) in the absence or presence of 400 μg/ml proteinase K (Life Technologies) for 60 min. Digestion was stopped using 5 mM phenylmethylsulfonyl fluoride (Thermo Scientific). Cells were then prepared for SDS-PAGE and immunoblot analysis for BB0238, FlaB (periplasmic control), and OspC (outer membrane control). To determine whether BB0238 was intrinsically resistant to proteinase K degradation, proteinase K accessibility assays were repeated in the presence and absence of 0.05% Triton X-100 (Promega).

Immunofluorescence assays (IFA) were also used to evaluate surface

accessibility of BB0238 on the spirochete. For IFA with permeabilized (fixed) cells, bacteria were prepared as described by Revel et al. (7). Bb297 or BbΔ*bb0238* spirochetes were collected at mid-logarithmic growth phase, washed with PBS-$MgCl_2$, and resuspended in PBS-$MgCl_2$ to 1.5×10^7 spirochetes/ml. Cells were spotted on a CSS-100 silylated slide (CEL Associates, Pearland, TX) and allowed to air dry. The slides were fixed at 65°C, followed by incubation in acetone. The fixed cells were washed three times in cold PBS-$MgCl_2$ and incubated with blocking buffer (PBS-$MgCl_2$ with 0.05% Tween 20 and 5% bovine serum albumin [BSA]). The slides were then washed with cold PBS-$MgCl_2$ and incubated with primary antibodies recognizing FlaB, OspA, and BB0238 diluted in blocking buffer at 1:1,000, 1:1, and 1:500, respectively. Finally, the slides were washed with cold PBS-$MgCl_2$ and incubated with Alexa Fluor-conjugated secondary antibodies diluted 1:600 in blocking buffer (i.e., Alexa Fluor 488 anti-rat, Alexa Fluor 594 anti-mouse, and Alexa Fluor 647 anti-chicken; Life Technologies). The slides were then washed with cold PBS-$MgCl_2$, and the coverslip was affixed with Mowiol (Sigma) and prepared for imaging. Nonpermeabilized (unfixed) cells were prepared as previously described (25). Briefly, 5×10^7 spirochetes of Bb297 or BbΔ*bb0238* were resuspended in 100 μl of blocking buffer (PBS-$MgCl_2$ with 10% fetal bovine serum [FBS] [Life Technologies]). Primary antibodies were applied to the cells as described above and incubated at room temperature. The cells were washed with blocking buffer, resuspended in blocking buffer, and spotted on a silylated slide. The cells were fixed with PBS-$MgCl_2$ containing 4% formaldehyde, washed, and incubated with blocking buffer containing secondary antibodies at the concentrations listed above. The slides were washed and fixed with PBS-$MgCl_2$ containing 4% formaldehyde, and the coverslip was affixed with Mowiol. Fluorescence microscopy was performed using a Ti-U microscope with a 60× oil immersion objective, and images were taken using a D5-QilMc digital camera (Nikon, Melville, NY).

To assess localization of BB0238 to the bacterial membrane, Triton X-114 phase partitioning was performed as described by Brooks et al. (26). Protein in the detergent (i.e., membrane) and aqueous fractions were precipitated, prepared for SDS-PAGE, and transferred to nitrocellulose and PVDF membranes. The presence of BB0238, OspC, and BB0796 in each fraction was determined by immunoblot analysis.

Additional whole-cell fractionation was performed as previously described (27, 28) to further separate the protoplasmic cylinder from the outer membrane and periplasmic fractions. In brief, 5×10^9 spirochetes were washed, resuspended in PBS with 1% Triton X-114, and incubated overnight at 4°C. Centrifugation at 20,000 × *g* for 30 min at 4°C resulted in protoplasmic cylinder isolation; the supernatant was then warmed to 37°C and centrifuged at 15,000 × *g* for 15 min at room temperature. The aqueous upper phase was separated from the lower, detergent phase, and the two phases were washed. The protoplasmic cylinders and the aqueous (periplasmic) and detergent (outer membrane) fractions were then prepared for SDS-PAGE and immunoblot analyses.

Proteomic analysis of native BB0238. Gel electrophoresis combined with liquid chromatography-tandem mass spectrometry (GeLC–MS-MS) analysis of SDS-PAGE protein bands was performed as previously described (29). Volumes of cell lysate equivalent to 5×10^7 bacteria for Bb297 or BbΔ*bb0238* were loaded in a gel lane of a 12.5% SDS-PAGE gel in duplicate. One portion of the gel was transferred to nitrocellulose, and BB0238 was detected by immunoblotting as described above. The second portion was stained with GelCode Blue Stain Reagent (Thermo Scientific) and prepared for proteomic analysis. To generate gel slices, the PAGE gel was overlaid on the immunoblot to localize the regions of the lanes that corresponded to BB0238. Peptides and proteins were identified from tandem MS (MS-MS) spectra by database searching using the Mascot search engine (Matrix Science, Boston, MA).

Statistical analyses. The ID_{50} values for Bb297, BbΔ*bb0238*, and Bb*bb0238*^{C} were calculated as described previously (30). Comparisons between the clones' ID_{50} values were made by using a probit regression model, where we assumed identical slopes in the response/log-dose relationship but different intercepts for each clone. Graphically, they manifest as dose-response curves with lateral shifts corresponding to the changes in intercept. Additionally, an overdispersion parameter was fitted to accommodate greater homogeneity in infection rates than would normally be permitted by the model.

Tissue infection rates were analyzed using Fisher's exact tests. Analysis of variance (ANOVA) models were used to compare clones with respect to qPCR measurements, and Tukey's procedure was used to perform pairwise comparisons. Student unpaired *t* tests were used to analyze qRT-PCR measurements. Finally, histopathologic scores were compared using Wilcoxon rank sum tests with adjustments for multiple comparisons made using Sime's procedure. For all analyses, *P* values of less than 0.05 were considered statistically significant. All analyses were performed using R software version 3.0.1 (R Foundation for Statistical Computing, Vienna, Austria) and SAS 9.3 (SAS Institute Inc., Cary, NC).

RESULTS

Inactivation of *bb0238* in *B. burgdorferi*. *bb0238* encodes a hypothetical protein on the chromosome of *B. burgdorferi* (6). BB0238 is approximately 30.4 kDa in size (i.e., 262 amino acids) and is predicted to contain a TPR structural motif. While a BLASTP search identified homologs of BB0238 in both Lyme disease (99 to 90% identity) and relapsing fever (54 to 56% identity) *Borrelia* spp., no homologs were identified in other bacterial species (31). To evaluate the contribution of this novel protein during mammalian infection, allelic exchange was used to create a *bb0238*-deficient mutant in which a portion of the *bb0238* ORF was replaced with a P*flgB-aphI* resistance marker. Wild-type Bb297 was electroporated with pJSB430A, a suicide vector containing regions flanking *bb0238* with a Kan^r cassette interrupting the ORF (Fig. 1A). Kan^r transformants were recovered, integration of P*flgB-aphI* into *bb0238* was confirmed via PCR (Fig. 1B), and PCR-based plasmid profiling confirmed the endogenous plasmid content of BbΔ*bb0238* (see Fig. S1 in the supplemental material). The BbΔ*bb0238* mutant failed to produce BB0238 protein when whole-cell lysates were probed with BB0238-specific rat antisera (Fig. 1C). To restore *bb0238* expression in BbΔ*bb0238*, the mutant was transformed with pJSB445A, a shuttle plasmid that contained *bb0238*, the 420-bp upstream region with the putative *bb0238* promoter, and a P*flgB-aadA* Strep^r resistance marker. PCR confirmed that the Bb*bb0238*^{C} clone contained an intact *bb0238* ORF (Fig. 1B) and that its endogenous plasmid profile was similar to that of Bb297 (see Fig. S1 in the supplemental material). Complementation of BbΔ*bb0238* with pJSB445A restored production of the BB0238 protein (Fig. 1C), suggesting that the 420-bp region upstream of the ORF contains the *bb0238* promoter.

To assess total protein differences in Bb297 and BbΔ*bb0238*, whole-cell lysates were separated by SDS-PAGE and stained with Sypro Ruby. Although two low-molecular-mass bands (i.e., <31 kDa) appeared to be altered between the parent strain and the *bb0238* mutant (see Fig. S2 in the supplemental material), the comparison revealed no major global differences in protein expression profiles. The identities of the proteins represented by these two bands are currently unknown, but the upper band, which has an approximate mass of 30 kDa and was present in Bb297, may possibly represent BB0238. *In vitro* growth curve analyses showed that BbΔ*bb0238* grew similarly to Bb297 at 37°C, and no gross morphological defects were noted when BbΔ*bb0238* was visualized by dark-field microscopy (data not shown). Addi-

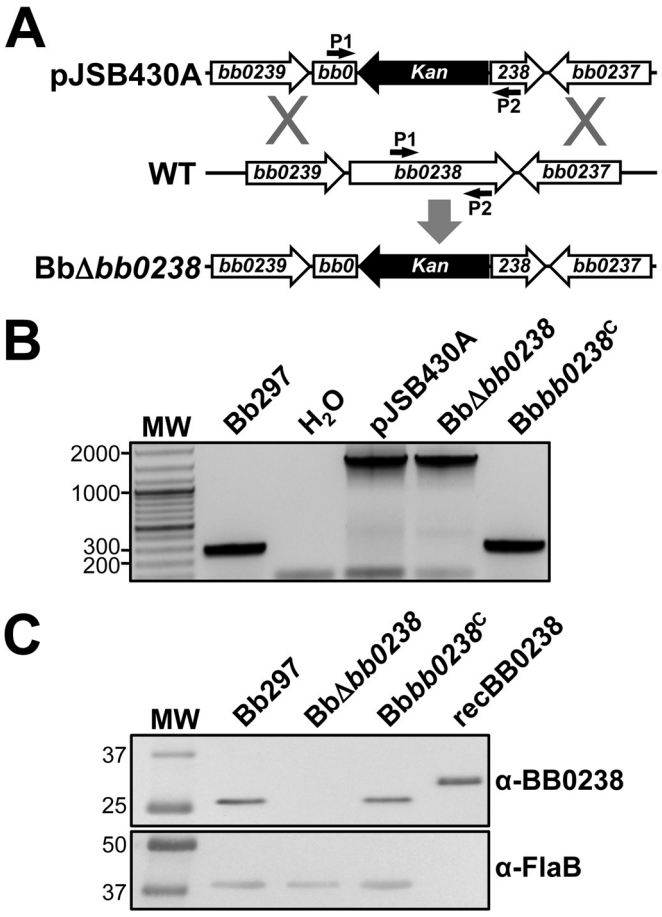

FIG 1 Generation and confirmation of BbΔ*bb0238* and the Bb*bb0238*^{C} complemented clone. (A) Diagram illustrating the approach to inactivating *bb0238* in Bb297. pJSB430A, relevant region of the *bb0238*::Kan mutagenesis construct; WT, *bb0238* and flanking regions from the *B. burgdorferi* chromosome; BbΔ*bb0238*, genomic arrangement of the *bb0238*::Kan mutant. The small arrows denote the relative positions of the *bb0238* P1 and P2 diagnostic primer pair. (B) PCR confirmation of the BbΔ*bb0238* mutant and complemented Bb*bb0238*^{C}. PCR with primers P1 and P2 results in different amplicon sizes, 287 bp (wild type) and 1,475 kb (*bb0238*::Kan). Bb297, wild-type *B. burgdorferi*; H_2O, negative control for amplification; pJSB430A, *bb0238*::Kan suicide vector used to interrupt *bb0238*. DNA size standards (lane MW), indicated on the left, are shown in kilobases. (C) Immunoblot analysis of BB0238 and FlaB in Bb297, BbΔ*bb0238*, and Bb*bb0238*^{C}. Antibodies used to detect the respective proteins are indicated on the right. recBB0238 denotes the lane containing His_6-tagged BB0238 recombinant protein used to generate antisera. The relevant molecular masses (kDa) of the standard (lane MW) are shown on the left.

tionally, swarm plate motility assays suggested that BbΔ*bb0238* exhibited no general motility defects (data not shown).

Requirement for *bb0238* during infection of mice. To determine the contribution of BB0238 to *B. burgdorferi* infection and pathogenesis, C3H/HeN mice were challenged via intradermal needle inoculation with increasing concentrations of *in vitro*-cultivated Bb297, BbΔ*bb0238*, or Bb*bb0238*^{C} (i.e., serial 10-fold dilutions from 10^2 to 10^5 bacteria). Ear punch, back skin, heart, bladder, tibiotarsal tissue, and lymph nodes were collected from mice at 2 weeks postinfection, and the tissues were cultured in BSK-II medium. The cultures were then examined by dark-field microscopy for the presence of spirochetes. Mice infected with BbΔ*bb0238* demonstrated a significant reduction in total numbers of culture-positive tissues, and this defect was not readily overcome by increasing the inoculum (Table 2). Interestingly, bacteria could not be recovered from ear punch biopsy specimens or heart tissues isolated from any of the BbΔ*bb0238*-infected mice. BbΔ*bb0238* also exhibited a defect in its capacity to infect tibiotarsal and bladder tissues, although this deficiency was partially alleviated upon inoculation of mice with higher doses of BbΔ*bb0238* (a maximum infection rate of 30% was observed at doses of 10^4 or 10^5 spirochetes). The infection rates in mice challenged with Bb*bb0238*^{C} were comparable to those of Bb297, suggesting the attenuation noted in BbΔ*bb0238* was specifically due to lack of BB0238. The ID_{50} of the BbΔ*bb0238* mutant was 1,507 spirochetes, which was comparable to those of Bb297 and Bb*bb0238*^{C} (i.e., 378 and 234 bacteria, respectively) (Table 2). However, this calculation was based on the number of infected mice and does not reflect the tissue-specific infection defect observed in mice challenged with BbΔ*bb0238*. To further assess the infectivity phenotype of BbΔ*bb0238*, a subset of tissue samples were analyzed via qPCR to measure spirochetal burdens in BbΔ*bb0238*-infected tissues (Fig. 2). qPCR results, reported as copies of *flaB* per 10^6 copies of mouse actin, showed significantly reduced spirochetal burdens in tissues from mice infected with BbΔ*bb0238*, even in culture-positive samples, compared to tissues isolated from mice infected with Bb297 and Bb*bb0238*^{C}. In agreement with these findings, histological scoring of heart and knee tissues also showed that the severity of carditis and arthritis, respectively, was significantly reduced in tissues collected from mice infected with BbΔ*bb0238* (Fig. 3). To confirm that *bb0238* is expressed during mammalian infection, five mice were infected with Bb297 at a dose of 10^5 bacteria, and total RNA was extracted from tissues at 14 days postinfection. *bb0238* transcripts, which were quantified using qRT-PCR and normalized to *flaB* (Fig. 4), were found to be similar between the six tissues tested. Although the elevated levels of *bb0238* in bacteria colonizing the heart and tibiotarsal tissue suggested that effective infection of these sites may require *bb0238*, the increase was relatively modest (i.e., only 2-fold higher) compared to other tissues.

It is well established that *B. burgdorferi* must evade the adaptive immune response to infect and disseminate in mice (32–38). To assess whether the attenuation of BbΔ*bb0238* is due to the mutant's inability to avoid clearance by adaptive immunity, *scid* mice were challenged via intradermal needle inoculation with 10^5 spirochetes of Bb297, BbΔ*bb0238*, or Bb*bb0238*^{C}. At 2 weeks postinoculation, tissues (i.e., ear punch, back skin, heart, bladder, and tibiotarsal) were isolated from infected mice and cultured in BSK-II. Examination of cultures inoculated with tissues from the *scid* mice infected with BbΔ*bb0238* revealed a reduction in culture-positive tissues (Table 3) comparable to that observed with BbΔ*bb0238*-infected C3H/HeN mice. Though all of the *scid* mice inoculated with BbΔ*bb0238* were infected, similar tissue-specific trends in attenuation were observed in C3H/HeN mice. Specifically, all of the ear punch cultures were negative, while only one heart was culture positive. In contrast to the results observed with the C3H/HeN mice, viable spirochetes were not recovered from any of the back skin cultures from the *scid* mice. In addition, BbΔ*bb0238* was able to infect the tibiotarsal tissues of *scid* mice more efficiently than those of C3H/HeN mice. The mice challenged with Bb*bb0238*^{C} were fully infected, confirming that the defect noted in BbΔ*bb0238*-infected mice is due to the lack of *bb0238*. Given that comparable reductions in infectivity were ob-

TABLE 2 Infectivity of the BbΔ*bb0238* mutant in C3H/HeN mice

Strain and dose (spirochetes)	No. of positive cultures/total							No. of infected mice/total	ID_{50}
	Ear punch	Back skin	Lymph nodes[a]	Heart	Tibiotarsal tissue	Bladder	All sites		
Bb297									
10^2	1/10	1/10	1/10	1/10	2/10	1/10	7/60	2/10	
10^3	5/10	6/10	7/10	7/10	9/10	7/10	41/60	9/10	378[b]
10^4	7/10	8/10	10/10	8/10	10/10	10/10	53/60	10/10	
10^5	7/10	10/10	10/10	7/10	10/10	10/10	54/60	10/10	
Bb*Δbb0238*									
10^2	0/10	2/10	2/10	0/10	1/10	1/10	6/60	2/10	
10^3	0/10[e]	4/10	4/10	0/10[e]	2/10[e]	0/10[e]	10/60[e]	4/10	1507[c,e]
10^4	0/10[e]	8/10	8/10	0/10[e]	3/10[e]	2/10[e]	21/60[e]	9/10	
10^5	0/10[e]	6/10	9/10	0/10[e]	2/10[e]	3/10[e]	20/60[e]	10/10	
Bb*bb0238*^{C}									
10^2	1/10	1/10	1/10	1/10	1/10	1/10	6/60	1/10	
10^3	3/10	4/10	4/10	4/10	7/10	3/10	25/60	7/10	234[d]
10^4	9/10	10/10	10/10	10/10	10/10	10/10	59/60	10/10	
10^5	7/10	10/10	10/10	10/10	10/10	10/10	57/60	10/10	

[a] A single brachial and inguinal lymph node were collected from each mouse and cultured together.
[b] 95% confidence interval (CI); range, 148 to 971 spirochetes.
[c] 95% CI; range, 617 to 3,690 spirochetes.
[d] 95% CI; range, 91 to 607 spirochetes.
[e] Statistically significant difference relative to Bb297 ($P < 0.05$).

served in both C3H/HeN and *scid* mice challenged with BbΔ*bb0238*, the attenuation of BbΔ*bb0238* does not appear to be solely due to the inability of the BbΔ*bb0238* spirochetes to avoid clearance via the adaptive immune response.

Characterization of *bb0238* gene architecture. Published annotation for *bb0238* provided limited information regarding the putative function of BB0238. However, the genes adjacent to *bb0238*, *bb0237* and *bb0239*, are predicted to encode an apolipoprotein, *N*-acyltransferase, and a deoxyguanosine/deoxyadenosine kinase, respectively (6). Since *bb0238* and *bb0237* are convergently transcribed, it is likely they do not comprise an operon (Fig. 5A). *bb0239* and *bb0238*, on the other hand, are oriented in the same direction on the chromosome with a relatively small intergenic region (45 bp), suggesting they may be cotranscribed. This is especially relevant considering that *bb0239* is predicted to be involved in *B. burgdorferi* purine salvage, and this pathway is essential for mammalian infection (39–41).

RT-PCR with RNA extracted from Bb297 was used to determine whether *bb0239* and *bb0238* comprised an operon. Primers that amplified a section internal to the *bb0238* ORF were employed, as well as a primer set that spanned the intergenic region (Fig. 5B). The *bb0238* internal primers generated an amplicon of the appropriate size, confirming the presence of *bb0238* transcripts, while the primer set spanning the *bb0239-bb0238* intergenic region did not yield a PCR product. Northern blot analysis was used to confirm the RT-PCR results and the size of the *bb0238* mRNA. Total RNA was extracted from Bb297 and BbΔ*bb0238* and hybridized with DIG-labeled probes recognizing *flaB* or *bb0238* transcripts. *flaB* transcripts were detected in both strains (Fig. 5C) at the correct size of ~1,100 bp (42, 43), thus confirming equal loading of sample. *bb0238* mRNA was detected only in Bb297, confirming the specificity of the probe. The *bb0238* transcript migrated at a size slightly smaller than the 1,059-bp band in the molecular weight standard. This agrees with an estimated size of a monocistronic *bb0238* transcript of ~800 bp. Finally, 5′ RACE was utilized to identify the transcription start site for the *bb0238* gene. Using a *bb0238*-specific primer that recognized a region 525 bp downstream of the start codon, 33 clones were isolated and sequenced. The amplified fragments from 16 of these 33 clones stopped within the *bb0238* ORF, suggesting they arose from premature termination of the extension reaction. Of the remaining 17 clones that mapped to a region upstream of the *bb0238* ORF, 12 mapped to a common TSS that was 37 bp upstream from the predicted start codon (Fig. 5A). The start sites in the remaining five fragments did not map to a common consensus residue. Based on this predicted start site, the *bb0238* transcript would be approximately 830 bp in length. Taken together, these data indicate that the promoter for *bb0238* lies within the predicted deoxyguanosine/deoxyadenosine gene *bb0239*, but these two genes are not operonic. Furthermore, these findings, in conjunction with the genetic complementation studies described above, confirm that the attenuated-infection phenotype observed in BbΔ*bb0238* is not likely due to a polar mutational effect on *bb0239* that arose from the insertion of the resistance marker in this mutant.

***In vitro* characterization of *bb0238* regulation.** To determine whether *bb0238* expression might differ during the *B. burgdorferi* enzootic life cycle, wild-type Bb297 was cultured *in vitro* under conditions that mimic the conditions with the mammal/fed tick (pH 6.8 and 37°C) and unfed tick (pH 7.5 and 23°C) (44–47). *bb0238* expression was analyzed via qRT-PCR (Fig. 6A) and immunoblotting (Fig. 6B). Although there was a modest change in *bb0238* mRNA expression under the two conditions, there was no demonstrable difference in the levels of BB0238 protein. To date, only one other study that described differential regulation of *bb0238* has been published. In this study, the authors detected an increase in *bb0238* transcription by comparative RNA sequencing

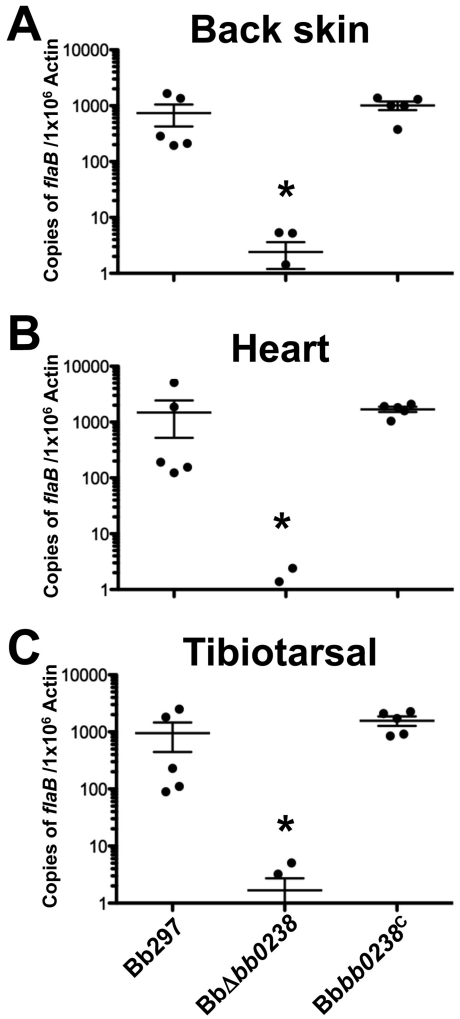

FIG 2 Spirochete burdens in tissues from mice infected with BbΔ*bb0238*. Tissues were collected 2 weeks postinfection from mice needle inoculated with Bb297, BbΔ*bb0238*, or Bb*bb0238*^{C} at a dose of 10^5 spirochetes. DNAs from tissue samples were analyzed in triplicate by qPCR to measure spirochete burdens. The results from back skin, heart, and tibiotarsal tissue are representative of a single infection experiment; $n = 5$ mice for each strain. The error bars represent standard errors of the mean (SEM). Statistical significance was determined by ANOVA and Tukey's procedure. The asterisks indicate a statistically significant difference relative to Bb297 or Bb*bb0238*^{C} ($P < 0.05$).

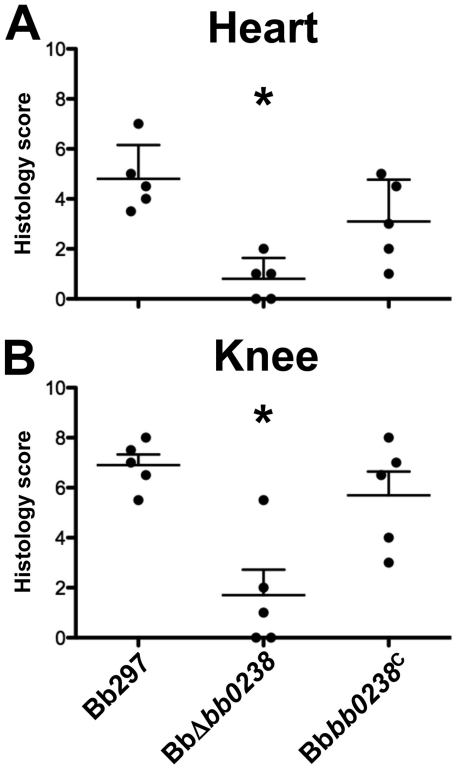

FIG 3 Histological evaluation of infected tissues. Heart and knee samples were collected 2 weeks postinfection from mice needle inoculated with Bb297, BbΔ*bb0238*, and Bb*bb0238*^{C} at a dose of 10^5 spirochetes. A blind histological assessment was performed, and disease severity scores from heart and knee are shown. The scores are representative of a single infection experiment; $n = 5$ mice for each strain. The error bars represent SEM. Statistical significance was determined using a Wilcoxon rank sum test with adjustments using Sime's procedure. The asterisks indicate a statistically significant difference relative to Bb297 or Bb*bb0238*^{C} ($P < 0.05$).

when the EbfC (YbaB) nucleoid-associated DNA-binding protein was overproduced (48). To confirm these results, the borrelial IPTG-inducible expression vector was adapted to express *ebfC* by replacing the *rrp2* ORF in piRrp2(Kan) with the *ebfC* ORF to create pJSB499. pJSB499 was transformed into Bb297, and the transformants, designated BbiEbfC, were recovered. A concentration of 1 mM IPTG was selected for induction because growth curve analyses determined that treatment of cultures of BbiEbfC with this concentration did not adversely affect growth (data not shown). Samples from the induced and uninduced BbiEbfC cultures were analyzed via qRT-PCR and immunoblotting for changes in expression. As expected, qRT-PCR showed over 10-fold increase in *ebfC* transcription (Fig. 6C). However, there was no significant increase in *bb0238* expression (Fig. 6C) or BB0238 protein levels (Fig. 6D). Prior studies showed that *dbpBA* transcription was elevated when *ebfC* was induced (48), and in agreement with these findings, DbpA production was higher in the samples from the IPTG-induced BbiEbfC cultures (Fig. 6D). Taken together, these data suggest that *bb0238* is not differentially expressed by *B. burgdorferi* during its enzootic cycle, nor is *bb0238* regulated by *ebfC*.

Determination of BB0238 cellular localization. Prediction using SignalP 4.1 suggested the N terminus of BB0238 contains either a transmembrane domain or a signal peptidase I cleavage site between amino acids 26 and 27 (19). Therefore, several assays were employed to determine where BB0238 is localized within the *B. burgdorferi* cell. First, a proteinase K accessibility assay was conducted to determine if BB0238 is exposed on the bacterial cell surface (Fig. 7A). When intact Bb297 cells were incubated with proteinase K, the OspC positive control was degraded due to surface localization. On the other hand, the FlaB negative control showed little to no degradation due to its protected location within the periplasmic space. Similar to FlaB, BB0238 was not degraded upon incubation of spirochetes with proteinase K. To confirm that BB0238 was not intrinsically resistant to degradation by proteinase K, spirochetes were permeabilized with Triton X-100 and then treated with proteinase K. BB0238, along with OspC and FlaB, were all readily degraded, confirming that BB0238 was sensitive to digestion by proteinase K. These results were sup-

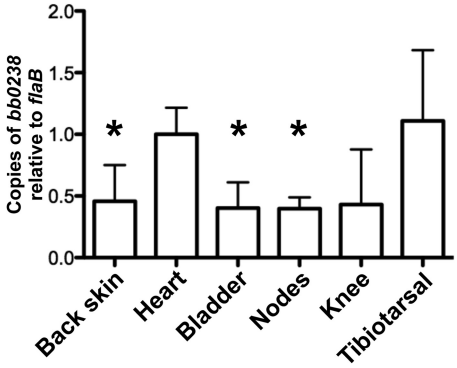

FIG 4 Expression of *bb0238* by spirochetes in infected murine tissues. RNA was isolated from tissues collected 2 weeks postinfection from mice needle inoculated with Bb297 at a dose of 10^5 spirochetes. Samples were analyzed in triplicate by qRT-PCR to quantify *bb0238* expression. The results are representative of a single infection experiment; $n = 5$ mice. The error bars represent SEM. Statistical significance was determined using an unpaired Student *t* test. The asterisks indicate a statistically significant difference relative to heart or tibiotarsal tissue ($P < 0.05$).

ported by microscopic IFAs with fixed (permeabilized) and unfixed (nonpermeabilized) spirochetes (Fig. 7B). The outer surface protein OspA could be detected in assays with both fixed and unfixed cells, while the periplasmic FlaB could be detected only in cells that had been fixed prior to incubation with antibody. BB0238 could not be detected in unfixed cells, suggesting subsurface localization, supporting the proteinase K results. The absence of a signal with Bb*Δbb0238* cells confirmed the specificity of the BB0238-specific antisera.

To further examine localization, BB0238 was analyzed by whole-cell phase partitioning, which separates fractions based on their amphiphilic properties (i.e., membrane localization). Bb297 was sonicated, incubated in Triton X-114, and separated into the detergent (membrane-enriched) and aqueous (non-membrane-enriched) fractions. Immunoblot analysis was then used to detect the presence of the proteins of interest (Fig. 7C), OspC, BB0796, and BB0238. BB0796 is a soluble aqueous-phase control described by Lenhart et al. (23). As expected, OspC, a known outer surface lipoprotein, was found in the detergent fraction, and BB0796 was detected in the aqueous fraction. BB0238 was enriched in the detergent fraction, which suggested association of BB0238 with the membrane. Cellular fractionation was utilized to more finely assess localization to the outer membrane, periplasmic space, or protoplasmic cylinder fractions (inner membrane and cytoplasm) (Fig. 7D). Fractions prepared from Bb297 were analyzed via immunoblot analyses. As expected, OspA was found in the outer membrane and protoplasmic cylinder fractions, and FlaB was detected in the protoplasmic cylinder. Like FlaB, BB0238 was also found in the protoplasmic cylinder fraction, suggesting either inner membrane or cytoplasmic localization. Given that the phase-partitioning data suggest BB0238 is membrane associated but cellular fractionation shows that BB0238 is localized to the protoplasmic cylinder, it is likely that BB0238 is associated with the inner membrane. However, these techniques do not distinguish whether BB0238 is anchored in the inner membrane or secreted into the periplasmic space and associated with the outer leaflet of the inner membrane. In an attempt to distinguish between these two possibilities, the mature BB0238 protein in a whole-cell lysate of Bb297 was analyzed by GeLC–MS-MS. A total of 217 proteins were identified in the excised gel slice, and BB0238 was the protein with the second highest relative abundance in the sample (data not shown). A total of 274 spectra that mapped to BB0238 were identified, with 81% coverage of the protein, but no peptides that mapped to the N-terminal 26 amino acids of the predicted BB0238 ORF were identified (Fig. 8). Since this portion of BB0238 seems to be absent in the mature protein, it is likely that BB0238 is secreted into the periplasm and is physically associated with the outer leaflet of the inner membrane directly or via interaction with another inner-membrane-associated protein.

Contribution of the putative TPR domain to BB0238 function. The fact that *bb0238* encodes a conserved hypothetical protein with no homology to proteins with known functions provides limited information regarding the mechanism by which it may contribute to mammalian infection. The original annotation of BB0238 on the Comprehensive Microbial Resource website (49) identified a putative TPR domain as the only functional motif within BB0238. The TPR motif is a structural domain that is associated with protein-protein interaction for proteins such as chaperones or protein transporters (13, 50, 51). The TPR domain consists of two α-helices that fold in an antiparallel fashion. Most TPR-containing proteins have multiple TPR domains that combine to create a binding cleft, though proteins with as few as one motif have been identified, as seen in BB0238. TPRpred (52) identified a single TPR domain between amino acids 40 and 73 ($P = 7.2 \times 10^{-5}$). Although the probability that this region functions as a TPR had limited predicted probability (<1%), comparison of the predicted TPR domain in BB0238 with a consensus TPR sequence shows alignment of key residues needed for secondary-structure formation and interaction (Fig. 9A) (13). To determine whether this domain contributed to BB0238 function, five *bb0238* mutants were generated with single point mutations of conserved residues in the TPR domain, three residing in helix A (Y43A, G47V, and Y50A) and two in helix B (A66G and P71A) (Fig. 9B). Point mutations were introduced in the TPR domain by overlap extension PCR, and the mutated *bb0238* was cloned into the pJSB201 borrelial shuttle vector to generate complementation vectors expressing each mutated ORF under the control of the

TABLE 3 Infectivity of the Bb*Δbb0238* mutant in *scid* mice

Strain	No. of positive cultures/total						No. positive mice/total
	Ear punch	Back skin	Heart	Tibiotarsal tissue	Bladder	All sites	
Bb297	5/5	3/5	5/5	5/5	3/5	21/25	5/5
Bb*Δbb0238*	0/5[a]	0/5	1/5[a]	5/5	1/5	7/25[a]	5/5
Bb*bb0238*^{C}	5/5	3/5	5/5	5/5	5/5	23/25	5/5

[a] Statistically significant difference relative to Bb297 ($P < 0.05$).

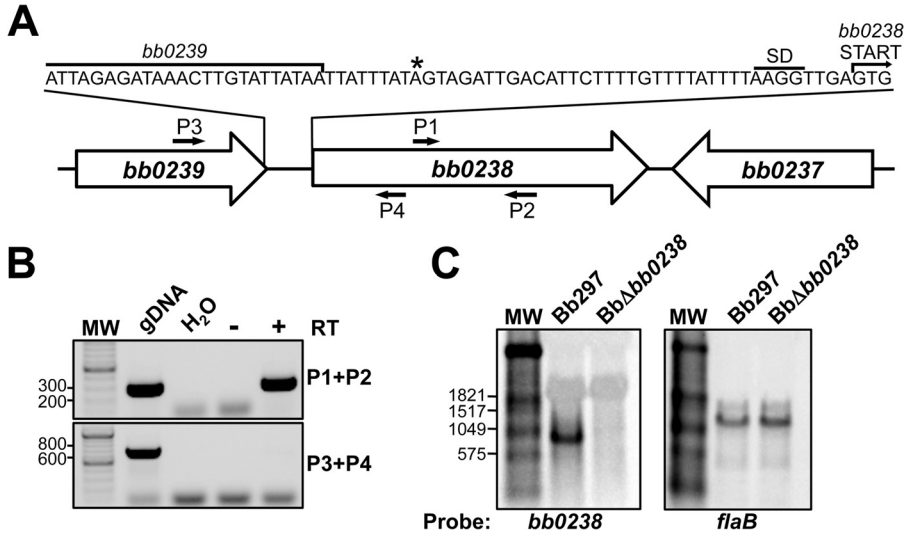

FIG 5 Analysis of the *bb0238* transcript. (A) Diagram illustrating *bb0238* linkage primer sites and TSS mapped by 5′ RACE. The small arrows denote the relative positions of *bb0238* diagnostic primers (P1 and P2) and *bb0238-bb0239* linkage primers (P3 and P4). The asterisk denotes the TSS predicted by 5′ RACE. (B) RT-PCR results with the *bb0238* internal control primers (P1 and P2) and linkage primers spanning the *bb0238* and *bb0239* intergenic region (P3 and P4). gDNA, Bb297 DNA; H_2O, negative control for amplification; for Bb297 RNA, − and + designate the reactions prepared without and with reverse transcriptase (RT), respectively. DNA size standards (lane MW), indicated to the left of the panel, are shown in base pairs. (C) Northern blot analysis of Bb297 and Bb*Δbb0238* RNAs. The probes and transcripts detected are indicated beneath the gels. Relevant sizes of the DIG-labeled RNA standard (lanes MW) are shown on the left in base pairs.

native *bb0238* promoter. Each complementation construct was then transformed into Bb*Δbb0238*, and BB0238 production was evaluated in the mutants by immunoblotting. BB0238 was detectable in Bb*bb0238*$_{Y43A}$, Bb*bb0238*$_{Y50A}$, Bb*bb0238*$_{A66G}$, and Bb*bb0238*$_{P71A}$ and present at levels comparable to those in Bb297 and Bb*bb0238*^{C}. Bb*bb0238*$_{G47V}$, on the other hand, did not produce BB0238 (Fig. 9C). qRT-PCR showed that *bb0238* transcript levels for all TPR mutants were equivalent to those measured in Bb*bb0238*^{C} (data not shown); therefore, the lack of BB0238 in Bb*bb0238*$_{G47V}$ is likely due to protein instability.

To evaluate the impacts of these TPR point mutations on BB0238 function during infection, C3H/HeN mice were challenged with Bb*bb0238*$_{Y43A}$, Bb*bb0238*$_{Y50A}$, Bb*bb0238*$_{A66G}$, and Bb*bb0238*$_{P71A}$ via intradermal needle inoculation with 10^5 bacte-

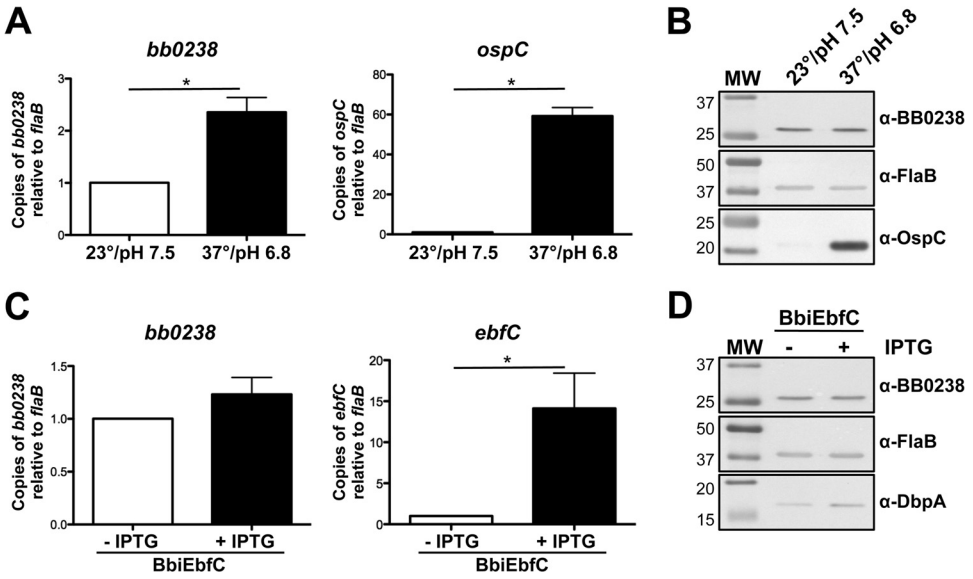

FIG 6 Regulation of *bb0238*. (A and B) qRT-PCR (A) and immunoblot analysis (B) of *bb0238* expression in Bb297 cultivated to mid-exponential growth phase at 23°C, pH 7.5, or grown to the late exponential growth phase at 37°C, pH 6.8. (C and D) qRT-PCR (C) and immunoblot analysis (D) of *bb0238* expression in BbiEbfC without IPTG or induced with 1 mM IPTG for 48 h. Detection of OspC protein and *ospC* transcript was used as a positive control to confirm *rpoS* activation. Detection of DbpA protein and *ebfC* transcript was included as a positive control to confirm *ebfC* expression. Relevant protein molecular masses (lane MW) are shown on the left in kDa. The immunoblot results are representative of two independent experiments. The qRT-PCR results are based on data from three biological replicates. The error bars represent SEM. Statistical significance was determined using an unpaired Student *t* test. The asterisks indicate a statistically significant difference between the respective conditions ($P < 0.05$).

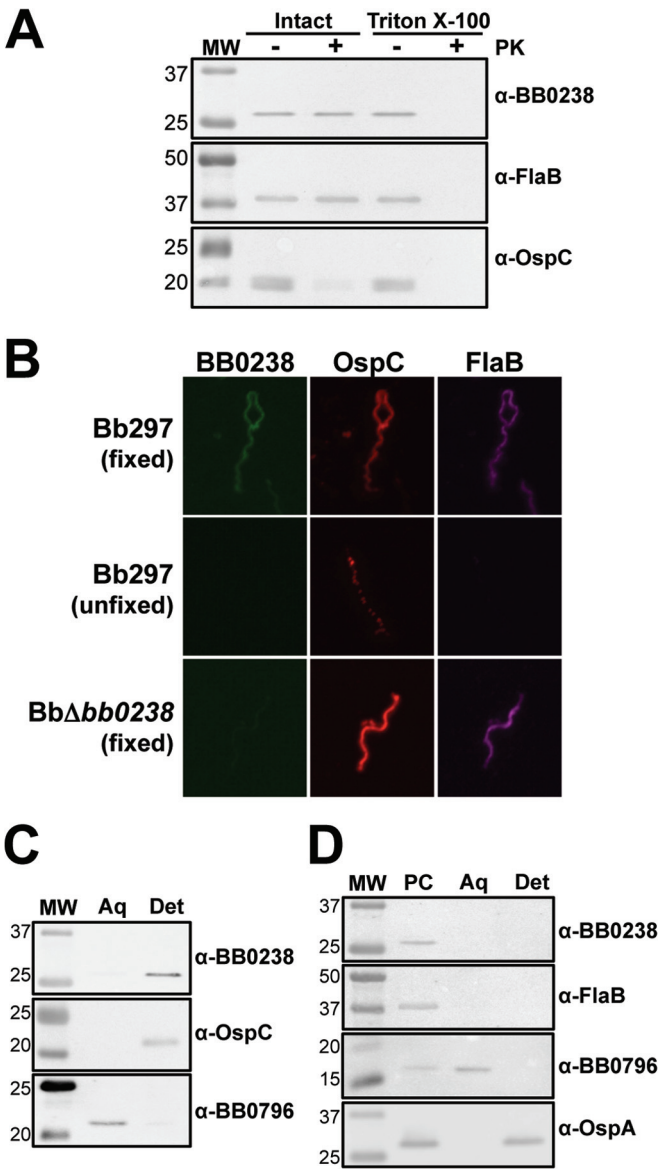

FIG 7 Cellular localization of BB0238. (A) Immunoblot analysis of the proteinase K accessibility assay. Bb297 cells were incubated with or without proteinase K (PK) in the presence or absence of Triton X-100. Antibodies to detect the respective proteins are listed on the right, and the relevant molecular masses (lane MW) are shown on the left in kDa. FlaB, negative control; OspC, positive control. (B) IFA of Bb297 and BbΔ*bb0238*. Fixed, cells were fixed to glass slides by air drying, heated, and then incubated in acetone; the slides were blocked and incubated with primary antibody and then secondary antibody. Unfixed, cells were incubated with primary antibody and then washed and fixed to glass slides with formaldehyde; the slides were then incubated with secondary antibody. Secondary antibodies for detection of BB0238, OspA, and FlaB were anti-rat Alexa Fluor 488, anti-mouse Alexa Fluor 594, and anti-chicken Alexa Fluor 647, respectively. (C) Immunoblot analysis of whole-cell phase partitioning. Bb297 cells were phase separated into aqueous (Aq) and detergent (Det) fractions. Antibodies to detect the respective proteins are listed on the right, and the relevant molecular masses (lane MW) are shown on the left in kDa. OspC was used as a control for the membrane-localized, detergent-enriched fraction, and detection of BB0796 was used as an aqueous control. (D) Immunoblot analysis of cellular fractionation. Bb297 cells were incubated with Triton X-114. The protoplasmic cylinder (PC) was pelleted, and samples were incubated at 37°C for phase separation. The aqueous (Aq) and detergent (Det) fractions were then separated. Antibodies to detect the respective proteins are listed on the right, and the relevant molecular masses (lane MW) are shown on the left in kDa. FlaB was used as a protoplasmic cylinder control, periplasmic BB0796 as an aqueous control, and outer-membrane-localized OspA as a detergent control. The data shown are representative blots from a minimum of two independent experiments.

ria. Because Bb*bb0238*$_{G47V}$ did not produce the BB0238 protein, the clone was excluded from the infection experiments, as it would presumably have the same phenotype as BbΔ*bb0238*. The Bb*bb0238*$_{Y43A}$, Bb*bb0238*$_{Y50A}$, Bb*bb0238*$_{A66G}$, and Bb*bb0238*$_{P71A}$ TPR mutants were confirmed to contain all Bb297 endogenous plasmids known to be important for infection; Bb*bb0238*$_{Y50A}$ and Bb*bb0238*$_{A66G}$ were missing lp38 (see Fig. S1 in the supplemental material), but lp38 is not required by *B. burgdorferi* during the enzootic cycle (53). Ear punch, back skin, heart, bladder, tibiotarsal tissue, and lymph nodes were collected from mice at 2 weeks postinfection, and the tissues were cultured in BSK-II medium. The cultures were then examined by dark-field microscopy for the presence of spirochetes. Relative to Bb297 and Bb*bb0238*^{C}, Bb*bb0238*$_{Y43A}$, Bb*bb0238*$_{A66G}$, and Bb*bb0238*$_{P71A}$ demonstrated reduced tissue infection rates and attenuation comparable to that of BbΔ*bb0238* (Table 4). As noted in earlier experiments (Table 2), the total numbers of infected mice in each group were similar, but tissue-specific attenuation was observed in mice infected with BbΔ*bb0238*, Bb*bb0238*$_{Y43A}$, Bb*bb0238*$_{A66G}$, and Bb*bb0238*$_{P71A}$. Interestingly, there was an increase in the incidence of positive heart tissues for Bb*bb0238*$_{Y50A}$ compared to BbΔ*bb0238* and the other three TPR mutant clones. The results from the qPCR analysis of spirochetal burdens in tissues from infected mice showed trends similar to those in the culture data (Fig. 10). Tissues from mice infected with Bb*bb0238*$_{Y43A}$, Bb*bb0238*$_{A66G}$, and Bb*bb0238*$_{P71A}$ showed bacterial burdens comparable to those of BbΔ*bb0238* in all tissues tested. In agreement with the infectivity results, Bb*bb0238*$_{Y50A}$ was present in the heart tissues at nearly wild-type levels. In addition, the mutant also showed bacterial numbers equivalent to those of Bb297 and Bb*bb0238*^{C} in back skin tissues. However, bacterial burdens in tibiotarsal tissues from mice infected with Bb*bb0238*$_{Y50A}$ were reduced to levels similar to those detected in BbΔ*bb0238*. While the exact function of BB0238 remains unknown, these data suggest that several of these conserved residues in the putative TPR domain are important for BB0238 function.

DISCUSSION

Given the high percentage of hypothetical proteins present in the genome of *B. burgdorferi* (6), characterization of genes of unknown function could help define the molecular mechanisms of host-pathogen interactions and identify new targets for disease intervention. While we were unable to define the function of BB0238 in *B. burgdorferi* and its specific role in virulence remains unknown, this study provides sufficient evidence to conclude that it is required for efficient infection in the murine infection model. The *bb0238* mutant exhibited significant attenuation during experimental mammalian infection. This defect, characterized by reduced infection in specific tissues, most notably the heart and ear tissues (Table 2 and Fig. 2), could not be diminished even when the inoculum was increased significantly above the parental ID_{50}. Though there were substantial decreases in tissue spirochete burdens and a large number of culture-negative tissues, the total number of mice infected by BbΔ*bb0238* remained similar to the

MLMEVLMRRL FLLYILCSFV FLNLFA**Q**GSS SYIDK**Q**KELA IFYYEVGQRY INVGKIKKGK LFQAKALKIY
PDLKKGFDIK LAVKELDARI KDDNPKVV**M**L EDIKLEEIPG IVHEKIEIND FTNAPKIEYI A**Q**RERSKN**Q**D
KIIKFQFGKF ARALISRNFD LFDSVIADKV NV**M**GQFESKN DFISTLSSAS SKADADELEY LSVDDYYDLK
SLKISKSNDT SFAVNVNAKK NDVTKNFPFW KER**Q**TLIFTT EDDNNWFLSS IN

FIG 8 Analysis of mature BB0238 in Bb297 by GeLC–MS-MS. The amino acid sequence for BB0238 is shown, with underlining indicating regions of the protein for which peptides were detected. Boldface indicates amino acids that were oxidized or pryomodified. The arrow indicates the signal peptide cleavage site predicted by SignalP. The findings represent the results obtained from analysis of two biological replicates.

total number of mice infected by Bb297. As a result, only a modest increase in the ID_{50} for BbΔ*bb0238* was observed. Reduced infection rates in the tibiotarsal joints of BbΔ*bb0238*-infected mice were not a consistent phenotype across infection experiments and models. However, in experiments where higher infection rates were detected, the spirochete burden in these tissues was always significantly lower than for the wild type. The inability of BbΔ*bb0238* to infect immunocompromised *scid* mice suggests that the *bb0238* mutant is not attenuated solely because it was unable to evade the adaptive immune response (Table 3). It is worth noting that all infection analyses in mice were conducted at 2 weeks postchallenge, and it is possible that the observed defect may be overcome during long-term infections. Additionally, the mammalian infection model evaluates only one side of the *B. burgdorferi* life cycle. Given that *bb0238* is expressed under conditions mimicking the unfed tick and fed tick (Fig. 6A and B), one would expect *bb0238* to be expressed by bacteria during both tick colonization and transmission to the mammal. Upon evaluation of BbΔ*bb0238* in the tick and during vector-mediated transmission, it may be found that *bb0238* also plays a role during these events.

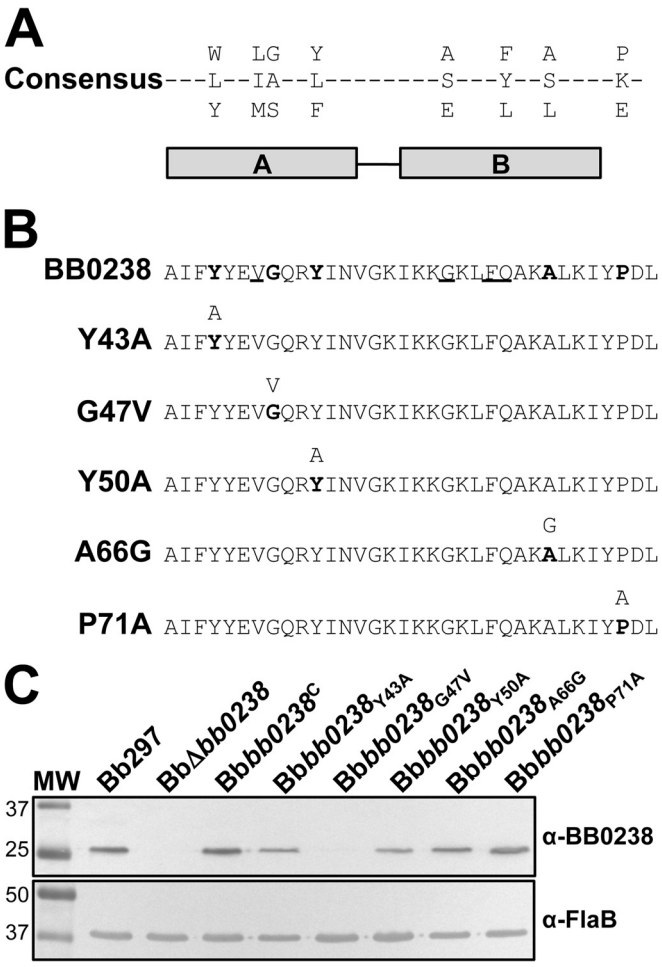

FIG 9 Characterization of BB0238 TPR point mutants. (A) Consensus sequence of the TPR motif predicted from sequence alignment of known TPR-containing proteins (13). The horizontal bars below the alignment indicate helices A and B. (B) BB0238 predicted TPR region (residues 40 to 73), with consensus residues in boldface and conserved residues underlined. The TPR mutations engineered in BB0238 are shown below the parental sequence, with the targeted residue(s) in boldface and the mutated residue above. (C) Immunoblot analysis of BB0238 expression in Bb297, BbΔ*bb0238*, Bb*bb0238*^{C}, Bb*bb0238*$_{Y43A}$, Bb*bb0238*$_{G47V}$, Bb*bb0238*$_{Y50A}$, Bb*bb0238*$_{A66G}$, and Bb*bb0238*$_{P71A}$ assessing protein expression of native and mutated BB0238. Detection of FlaB was included as a loading control. The relevant molecular weight markers (lane MW) are noted on the left. The immunoblot results are representative data from two independent experiments.

Because the *bb0238* mutant was specifically unable to infect the heart and ear tissue (Table 2), we wanted to determine if *bb0238* was differentially regulated by bacteria within different mammalian tissues (Fig. 4). In agreement with these findings, a minor increase in the levels of *bb0238* transcripts was detected in heart tissues. A similar increase in *bb0238* expression was observed in the tibiotarsal tissues, which also correlated with reduced infection rates in BbΔ*bb0238*-infected mice. It is possible that variations within tissue microenvironments (i.e., unknown host stimuli or nutrient availability) trigger a change in *bb0238* expression, but the changes among tissues were relatively modest (approximately 2-fold). Although the *in vitro* expression data determined that *bb0238* was not differentially regulated (Fig. 6A and B), it is likely that the *in vitro* culture conditions do not fully recapitulate the complex environments within the tick or vertebrate host. Therefore, comparison of *bb0238* transcription in the vector and host during each stage of the enzootic cycle is necessary to fully confirm that *bb0238* is constitutively expressed by *B. burgdorferi*.

Cellular localization assays suggest that BB0238 fractionates to the inner membrane (Fig. 7), and SignalP predicted that the N terminus of BB0238 may contain either a transmembrane domain or a signal peptidase I cleavage site. Since the proteomic analysis of mature BB0238 was unable to identify a peptide mapping to the region containing the predicted signal peptide (Fig. 8), it is likely that BB0238 is secreted into the periplasm and is associated with some component of the inner membrane. In addition, the subsurface localization of BB0238 suggests that it does not directly interact with mammalian proteins. Therefore, the attenuated infectivity in the *bb0238* mutant is not due to the inability of BbΔ*bb0238* to interact with extracellular matrix host proteins, unless BB0238 aids in export of such proteins to the cell surface. Because *B. burgdorferi* encodes other proteins that contain TPR domains, it is possible that one of these other TPR-containing proteins may compensate to a lesser degree for the lack of BB0238 in certain tissues of the mam-

TABLE 4 Infectivity of *B. burgdorferi bb0238* TPR mutants in C3H/HeN mice

Strain	No. of positive cultures/total							No. positive mice/total
	Ear punch	Back skin	Lymph nodes[a]	Heart	Tibiotarsal tissue	Bladder	All sites	
Bb297	5/5	5/5	5/5	5/5	5/5	5/5	30/30	5/5
BbΔ*bb0238*	0/5[b]	5/5	5/5	1/5[b]	3/5	0/5[b]	14/30[b]	5/5
Bb*bb0238*^{C}	5/5	5/5	5/5	5/5	5/5	5/5	30/30	5/5
Bb*bb0238*$_{Y43A}$	0/5[b]	3/5	1/5[b]	1/5[b]	3/5	0/5[b]	8/30[b]	4/5
Bb*bb0238*$_{Y50A}$	0/5[b]	3/5	5/5	5/5	3/5	2/5	18/30[b]	5/5
Bb*bb0238*$_{A66G}$	0/5[b]	2/5	2/5	0/5[b]	3/5	1/5[b]	8/30[b]	3/5
Bb*bb0238*$_{P71A}$	0/5[b]	3/5	2/5	0/5[b]	3/5	1/5[b]	9/30[b]	4/5

[a] A single brachial and inguinal lymph node were collected from each mouse and cultured together.
[b] Statistically significant difference relative to Bb*bb0238*^{C} ($P < 0.05$).

malian host (i.e., lymph nodes and back skin) during infection with the BbΔ*bb0238* mutant, thus explaining the tissue-specific attenuation in infection and bacterial burden. Results from swarm assays suggest that basic bacterial motility is not compromised in BbΔ*bb0238* and that it does not contribute to the infectivity defect (data not shown), though functionality of the chemosensory pathways has not been ruled out. Similarly, no growth defects were identified for BbΔ*bb0238 in vitro* (data not shown), but the attenuation could be due to the *bb0238* mutant's inability to obtain nutrients from the mammalian host. Considering that BSK-II is a nutrient-rich medium (15), it is possible that cultivation in this medium *in vitro* could likely mask growth defects that may be more apparent in the mammal. Cultivation of BbΔ*bb0238* within dialysis membrane chambers (DMC) implanted in rat peritoneal cavities could provide insight into a possible role for BB0238 in nutrient acquisition in the host. Though the DMC experiments do not address tissue-specific differences in nutrient requirements or availability, the experiments may identify a general *in vivo* growth defect that could result in the attenuated-infectivity phenotype similar to that seen with *pncA* (54). As noted above, the gene adjacent to *bb0239* is predicted to encode a deoxyguanosine/deoxyadenosine kinase involved in *B. burgdorferi* purine salvage, and this pathway is essential for mammalian infection (39, 40). Due to the physical proximity of *bb0238* and *bb0239* in the genome, it is possible that *bb0238* may play an ancillary role in purine salvage. Interestingly, attempts to disrupt *bb0239* in Bb297 were unsuccessful, suggesting *bb0239* may be essential for *B. burgdorferi* growth (data not shown).

Despite our limited knowledge regarding the function of *bb0238*, the original annotation of BB0238 on the Comprehensive Microbial Resource database identified several residues in the N-terminal region that matched the consensus for a TPR domain (13, 50). This putative TPR domain also appears to be functionally important for BB0238, as clones carrying point mutations engineered in the more highly conserved consensus residues either (i) did not express BB0238, presumably due to destabilization and degradation of the G47V mutant protein, or (ii) exhibited attenuated infectivity comparable to that observed in the *bb0238* deletion mutant (Table 4 and Fig. 9 and 10). BB0238 contains only one TPR motif, which is unusual among TPR motif-containing proteins, though examples of proteins in which a single TPR motif mediates protein-protein interactions exist (13, 50, 51). At this time, it still remains to be determined whether this region functions as an actual TPR domain, and the contribution of the domain to the physiological role of BB0238 remains unclear. It is possible that the point mutations generated in BB0238 could have altered the overall protein structure; however, attempts to generate soluble recombinant BB0238 protein for the purposes of structure-function analyses and nuclear magnetic resonance (NMR) structure characterization of the TPR mutants have been unsuccessful. If the TPR motif of BB0238 does indeed function as a prototypical protein-protein interaction domain, then BB0238 may be a chaperone, a common role for TPR-containing proteins. If BB0238 does act as a chaperone, it could be implicated in a number of physiological pathways, such as protein folding, protein transport, or chaperone-protease interactions.

Future studies will focus on delineating the function of BB0238. Given the presence and presumed importance of the TPR domain, attempts to identify a putative binding partner for BB0238 have high priority. Identification of a binding partner would not only shed light on a possible role for BB0238 in *B. burgdorferi* function, but would allow use of our TPR mutants in identifying relevant residues for protein-protein interactions. Additionally, all the infection analyses reported here were performed at 2 weeks postinfection. Analysis of BbΔ*bb0238* during long-term infections may determine whether the infectivity defect seen with the *bb0238* knockout is alleviated during chronic infection. Finally, the *bb0238* mutant should be evaluated throughout the rest of the experimental enzootic cycle to determine if BbΔ*bb0238* is able to colonize ticks and is competent for tick-to-mouse transmission. In conclusion, these studies have demonstrated that *bb0238* is required for efficient *B. burgdorferi* mammalian infection, but further experimentation is required to determine the precise contribution(s) of BB0238 during infection.

ACKNOWLEDGMENTS

This research was supported by funding to Jon S. Blevins through the Arkansas Biosciences Institute (a major research component of the Arkansas Tobacco Settlement Proceeds Act of 2000) and NIH/NIAID R01-AI087678, as well as support through the Translational Research Institute (UL1-TR000039; NIH National Center for Research Resources and National Center for Advancing Translational Sciences) and the UAMS Center for Microbial Pathogenesis and Host Inflammatory Responses (P20-GM103625).

We thank Daniel Voth for his assistance with microscopy and for the use of the microscope. We also thank Ricky Edmondson, Alan Tackett, and Samuel Mackintosh in the UAMS Proteomics Core and Allen Gies in the UAMS Sequencing Core Facility for their technical assistance. Finally, we thank Darrin Akins for providing the BB0796-specific antiserum used in these studies.

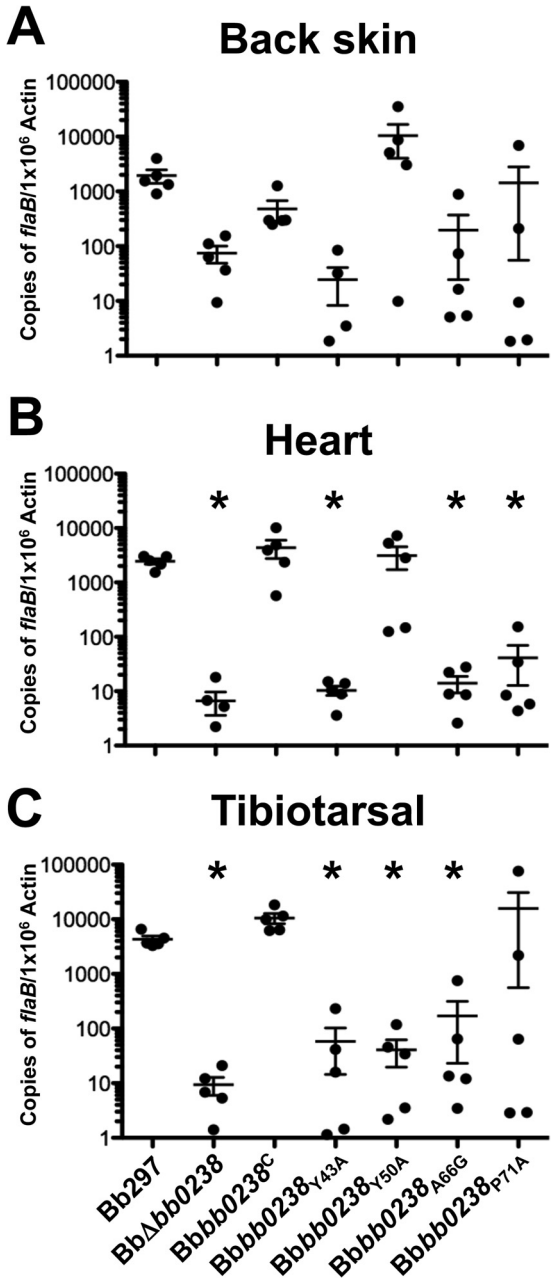

FIG 10 Spirochete burdens in tissues from mice infected with BB0238 TPR point mutants. Tissues were collected 2 weeks postinfection from mice needle inoculated with a dose of 10^5 spirochetes of Bb297, BbΔ*bb0238*, Bb*bb0238*^{C}, Bb*bb0238*$_{Y43A}$, Bb*bb0238*$_{Y50A}$, Bb*bb0238*$_{A66G}$, or Bb*bb0238*$_{P71A}$. DNAs from tissue samples were analyzed in triplicate by qPCR to measure spirochete burdens. The results from back skin, heart, and tibiotarsal tissue are representative of a single infection experiment ($n = 5$ mice for each strain). The error bars represent SEM. Statistical significance was determined using an unpaired Student *t* test. The asterisks indicate a statistically significant difference relative to Bb*bb0238*^{C} ($P < 0.05$).

REFERENCES

1. **Burgdorfer W, Barbour AG, Hayes SF, Benach JL, Grunwaldt E, Davis JP.** 1982. Lyme disease—a tick-borne spirochetosis? Science **216:**1317–1319. http://dx.doi.org/10.1126/science.7043737.
2. **Radolf JD, Caimano MJ, Stevenson B, Hu LT.** 2012. Of ticks, mice and men: understanding the dual-host lifestyle of Lyme disease spirochaetes. Nat. Rev. Microbiol. **10:**87–99. http://dx.doi.org/10.1038/nrmicro2714.
3. **Steere AC, Grodzicki RL, Kornblatt AN, Craft JE, Barbour AG, Burgdorfer W, Schmid GP, Johnson E, Malawista SE.** 1983. The spirochetal etiology of Lyme disease. N. Engl. J. Med. **308:**733–740. http://dx.doi.org/10.1056/NEJM198303313081301.
4. **Stanek G, Wormser GP, Gray J, Strle F.** 2012. Lyme borreliosis. Lancet **379:**461–473. http://dx.doi.org/10.1016/S0140-6736(11)60103-7.
5. **Steere AC, Coburn J, Glickstein L.** 2004. The emergence of Lyme disease. J. Clin. Invest. **113:**1093–1101. http://dx.doi.org/10.1172/JCI200421681.
6. **Fraser CM, Casjens S, Huang WM, Sutton GG, Clayton R, Lathigra R, White O, Ketchum KA, Dodson R, Hickey EK, Gwinn M, Dougherty B, Tomb JF, Fleischmann RD, Richardson D, Peterson J, Kerlavage AR, Quackenbush J, Salzberg S, Hanson M, van Vugt R, Palmer N, Adams MD, Gocayne J, Weidman J, Utterback T, Watthey L, McDonald L, Artiach P, Bowman C, Garland S, Fuji C, Cotton MD, Horst K, Roberts K, Hatch B, Smith HO, Venter JC.** 1997. Genomic sequence of a Lyme disease spirochaete, *Borrelia burgdorferi*. Nature **390:**580–586. http://dx.doi.org/10.1038/37551.
7. **Revel AT, Blevins JS, Almazan C, Neil L, Kocan KM, de la Fuente J, Hagman KE, Norgard MV.** 2005. *bptA* (*bbe16*) is essential for the persistence of the Lyme disease spirochete, *Borrelia burgdorferi*, in its natural tick vector. Proc. Natl. Acad. Sci. U. S. A. **102:**6972–6977. http://dx.doi.org/10.1073/pnas.0502565102.
8. **Zhang X, Yang X, Kumar M, Pal U.** 2009. BB0323 function is essential for *Borrelia burgdorferi* virulence and persistence through tick-rodent transmission cycle. J. Infect. Dis. **200:**1318–1330. http://dx.doi.org/10.1086/605846.
9. **Yang X, Hegde S, Shroder DY, Smith AA, Promnares K, Neelakanta G, Anderson JF, Fikrig E, Pal U.** 2013. The lipoprotein La7 contributes to *Borrelia burgdorferi* persistence in ticks and their transmission to naive hosts. Microbes Infect. **15:**729–737. http://dx.doi.org/10.1016/j.micinf.2013.06.001.
10. **Kumar M, Yang X, Coleman AS, Pal U.** 2010. BBA52 facilitates *Borrelia burgdorferi* transmission from feeding ticks to murine hosts. J. Infect. Dis. **201:**1084–1095. http://dx.doi.org/10.1086/651172.
11. **Promnares K, Kumar M, Shroder DY, Zhang X, Anderson JF, Pal U.** 2009. *Borrelia burgdorferi* small lipoprotein Lp6.6 is a member of multiple protein complexes in the outer membrane and facilitates pathogen transmission from ticks to mice. Mol. Microbiol. **74:**112–125. http://dx.doi.org/10.1111/j.1365-2958.2009.06853.x.
12. **Patton TG, Dietrich G, Dolan MC, Piesman J, Carroll JA, Gilmore RD, Jr.** 2011. Functional analysis of the *Borrelia burgdorferi bba64* gene product in murine infection via tick infestation. PLoS One **6:**e19536. http://dx.doi.org/10.1371/journal.pone.0019536.
13. **Blatch GL, Lassle M.** 1999. The tetratricopeptide repeat: a structural motif mediating protein-protein interactions. Bioessays **21:**932–939.
14. **Hughes CA, Kodner CB, Johnson RC.** 1992. DNA analysis of *Borrelia burgdorferi* NCH-1, the first north central U.S. human Lyme disease isolate. J. Clin. Microbiol. **30:**698–703.
15. **Pollack RJ, Telford SR, Spielman A.** 1993. Standardization of medium for culturing Lyme disease spirochetes. J. Clin. Microbiol. **31:**1251–1255.
16. **Blevins JS, Hagman KE, Norgard MV.** 2008. Assessment of decorin-binding protein A to the infectivity of *Borrelia burgdorferi* in the murine models of needle and tick infection. BMC Microbiol. **8:**82. http://dx.doi.org/10.1186/1471-2180-8-82.
17. **Groshong AM, Gibbons NE, Yang XF, Blevins JS.** 2012. Rrp2, a prokaryotic enhancer-like binding protein, is essential for viability of *Borrelia burgdorferi*. J. Bacteriol. **194:**3336–3342. http://dx.doi.org/10.1128/JB.00253-12.
18. **Blevins JS, Revel AT, Smith AH, Bachlani GN, Norgard MV.** 2007. Adaptation of a luciferase gene reporter and *lac* expression system to *Borrelia burgdorferi*. Appl. Environ. Microbiol. **73:**1501–1513. http://dx.doi.org/10.1128/AEM.02454-06.
19. **Petersen TN, Brunak S, von Heijne G, Nielsen H.** 2011. SignalP 4.0: discriminating signal peptides from transmembrane regions. Nat. Methods **8:**785–786. http://dx.doi.org/10.1038/nmeth.1701.
20. **Maruskova M, Esteve-Gassent MD, Sexton VL, Seshu J.** 2008. Role of the BBA64 locus of *Borrelia burgdorferi* in early stages of infectivity in a murine model of Lyme disease. Infect. Immun. **76:**391–402. http://dx.doi.org/10.1128/IAI.01118-07.
21. **Bugrysheva JV, Godfrey HP, Schwartz I, Cabello FC.** 2011. Patterns and regulation of ribosomal RNA transcription in *Borrelia burgdorferi*. BMC Microbiol. **11:**17. http://dx.doi.org/10.1186/1471-2180-11-17.
22. **Yang X, Popova TG, Hagman KE, Wikel SK, Schoeler GB, Caimano MJ,**

Radolf JD, Norgard MV. 1999. Identification, characterization, and expression of three new members of the *Borrelia burgdorferi* Mlp (2.9) lipoprotein gene family. Infect. Immun. **67:**6008–6018.
23. **Lenhart TR, Kenedy MR, Yang X, Pal U, Akins DR.** 2012. BB0324 and BB0028 are constituents of the *Borrelia burgdorferi* beta-barrel assembly machine (BAM) complex. BMC Microbiol. **12:**60. http://dx.doi.org/10.1186/1471-2180-12-60.
24. **Blevins JS, Revel AT, Caimano MJ, Yang XF, Richardson JA, Hagman KE, Norgard MV.** 2004. The *luxS* gene is not required for *Borrelia burgdorferi* tick colonization, transmission to a mammalian host, or induction of disease. Infect. Immun. **72:**4864–4867. http://dx.doi.org/10.1128/IAI.72.8.4864-4867.2004.
25. **Bryksin AV, Tomova A, Godfrey HP, Cabello FC.** 2010. BmpA is a surface-exposed outer-membrane protein of *Borrelia burgdorferi*. FEMS Microbiol. Lett. **309:**77–83. http://dx.doi.org/10.1111/j.1574-6968.2010.02020.x.
26. **Brooks CS, Vuppala SR, Jett AM, Akins DR.** 2006. Identification of *Borrelia burgdorferi* outer surface proteins. Infect. Immun. **74:**296–304. http://dx.doi.org/10.1128/IAI.74.1.296-304.2006.
27. **Cunningham TM, Walker EM, Miller JN, Lovett MA.** 1988. Selective release of the *Treponema pallidum* outer membrane and associated polypeptides with Triton X-114. J. Bacteriol. **170:**5789–5796.
28. **Zhang H, Raji A, Theisen M, Hansen PR, Marconi RT.** 2005. *bdrF2* of Lyme disease spirochetes is coexpressed with a series of cytoplasmic proteins and is produced specifically during early infection. J. Bacteriol. **187:**175–184. http://dx.doi.org/10.1128/JB.187.1.175-184.2005.
29. **Zielinska AK, Beenken KE, Mrak LN, Spencer HJ, Post GR, Skinner RA, Tackett AJ, Horswill AR, Smeltzer MS.** 2012. *sarA*-mediated repression of protease production plays a key role in the pathogenesis of *Staphylococcus aureus* USA300 isolates. Mol. Microbiol. **86:**1183–1196. http://dx.doi.org/10.1111/mmi.12048.
30. **Jewett MW, Lawrence K, Bestor AC, Tilly K, Grimm D, Shaw P, VanRaden M, Gherardini F, Rosa PA.** 2007. The critical role of the linear plasmid lp36 in the infectious cycle of *Borrelia burgdorferi*. Mol. Microbiol. **64:**1358–1374. http://dx.doi.org/10.1111/j.1365-2958.2007.05746.x.
31. **Altschul SF, Wootton JC, Gertz EM, Agarwala R, Morgulis A, Schaffer AA, Yu YK.** 2005. Protein database searches using compositionally adjusted substitution matrices. FEBS J. **272:**5101–5109. http://dx.doi.org/10.1111/j.1742-4658.2005.04945.x.
32. **Barthold SW, Sidman CL, Smith AL.** 1992. Lyme borreliosis in genetically resistant and susceptible mice with severe combined immunodeficiency. Am. J. Trop. Med. Hyg. **47:**605–613.
33. **McKisic MD, Barthold SW.** 2000. T-cell-independent responses to *Borrelia burgdorferi* are critical for protective immunity and resolution of Lyme disease. Infect. Immun. **68:**5190–5197. http://dx.doi.org/10.1128/IAI.68.9.5190-5197.2000.
34. **Bockenstedt LK, Kang I, Chang C, Persing D, Hayday A, Barthold SW.** 2001. CD4+ T helper 1 cells facilitate regression of murine Lyme carditis. Infect. Immun. **69:**5264–5269. http://dx.doi.org/10.1128/IAI.69.9.5264-5269.2001.
35. **Schaible UE, Kramer MD, Museteanu C, Zimmer G, Mossmann H, Simon MM.** 1989. The severe combined immunodeficiency (scid) mouse. A laboratory model for the analysis of Lyme arthritis and carditis. J. Exp. Med. **170:**1427–1432.
36. **McKisic MD, Redmond WL, Barthold SW.** 2000. Cutting edge: T cell-mediated pathology in murine Lyme borreliosis. J. Immunol. **164:**6096–6099. http://dx.doi.org/10.4049/jimmunol.164.12.6096.
37. **Schaible UE, Gay S, Museteanu C, Kramer MD, Zimmer G, Eichmann K, Museteanu U, Simon MM.** 1990. Lyme borreliosis in the severe combined immunodeficiency (*scid*) mouse manifests predominantly in the joints, heart, and liver. Am. J. Pathol. **137:**811–820.
38. **Fikrig E, Barthold SW, Chen M, Grewal IS, Craft J, Flavell RA.** 1996. Protective antibodies in murine Lyme disease arise independently of CD40 ligand. J. Immunol. **157:**1–3.
39. **Jain S, Sutchu S, Rosa PA, Byram R, Jewett MW.** 2012. *Borrelia burgdorferi* harbors a transport system essential for purine salvage and mammalian infection. Infect. Immun. **80:**3086–3093. http://dx.doi.org/10.1128/IAI.00514-12.
40. **Jewett MW, Lawrence KA, Bestor A, Byram R, Gherardini F, Rosa PA.** 2009. GuaA and GuaB are essential for *Borrelia burgdorferi* survival in the tick-mouse infection cycle. J. Bacteriol. **191:**6231–6241. http://dx.doi.org/10.1128/JB.00450-09.
41. **Lawrence KA, Jewett MW, Rosa PA, Gherardini FC.** 2009. *Borrelia burgdorferi bb0426* encodes a 2′-deoxyribosyltransferase that plays a central role in purine salvage. Mol. Microbiol. **72:**1517–1529. http://dx.doi.org/10.1111/j.1365-2958.2009.06740.x.
42. **Ge Y, Old IG, Girons IS, Charon NW.** 1997. The *flgK* motility operon of *Borrelia burgdorferi* is initiated by a sigma 70-like promoter. Microbiology **143:**1681–1690. http://dx.doi.org/10.1099/00221287-143-5-1681.
43. **Noppa L, Burman N, Sadziene A, Barbour AG, Bergstrom S.** 1995. Expression of the flagellin gene in *Borrelia* is controlled by an alternative sigma factor. Microbiology **141:**85–93. http://dx.doi.org/10.1099/00221287-141-1-85.
44. **Revel AT, Talaat AM, Norgard MV.** 2002. DNA microarray analysis of differential gene expression in *Borrelia burgdorferi*, the Lyme disease spirochete. Proc. Natl. Acad. Sci. U. S. A. **99:**1562–1567. http://dx.doi.org/10.1073/pnas.032667699.
45. **Brooks CS, Hefty PS, Jolliff SE, Akins DR.** 2003. Global analysis of *Borrelia burgdorferi* genes regulated by mammalian host-specific signals. Infect. Immun. **71:**3371–3383. http://dx.doi.org/10.1128/IAI.71.6.3371-3383.2003.
46. **Ojaimi C, Brooks C, Casjens S, Rosa P, Elias A, Barbour A, Jasinskas A, Benach J, Katona L, Radolf J, Caimano M, Skare J, Swingle K, Akins D, Schwartz I.** 2003. Profiling of temperature-induced changes in *Borrelia burgdorferi* gene expression by using whole genome arrays. Infect. Immun. **71:**1689–1705. http://dx.doi.org/10.1128/IAI.71.4.1689-1705.2003.
47. **Yang X, Goldberg MS, Popova TG, Schoeler GB, Wikel SK, Hagman KE, Norgard MV.** 2000. Interdependence of environmental factors influencing reciprocal patterns of gene expression in virulent *Borrelia burgdorferi*. Mol. Microbiol. **37:**1470–1479. http://dx.doi.org/10.1046/j.1365-2958.2000.02104.x.
48. **Jutras BL, Bowman A, Brissette CA, Adams CA, Verma A, Chenail AM, Stevenson B.** 2012. EbfC (YbaB) is a new type of bacterial nucleoid-associated protein and a global regulator of gene expression in the Lyme disease spirochete. J. Bacteriol. **194:**3395–3406. http://dx.doi.org/10.1128/JB.00252-12.
49. **Davidsen T, Beck E, Ganapathy A, Montgomery R, Zafar N, Yang Q, Madupu R, Goetz P, Galinsky K, White O, Sutton G.** 2010. The comprehensive microbial resource. Nucleic Acids Res. **38:**D340–D345. http://dx.doi.org/10.1093/nar/gkp912.
50. **D'Andrea LD, Regan L.** 2003. TPR proteins: the versatile helix. Trends Biochem. Sci. **28:**655–662. http://dx.doi.org/10.1016/j.tibs.2003.10.007.
51. **Main ER, Jackson SE, Regan L.** 2003. The folding and design of repeat proteins: reaching a consensus. Curr. Opin. Struct. Biol. **13:**482–489. http://dx.doi.org/10.1016/S0959-440X(03)00105-2.
52. **Biegert A, Mayer C, Remmert M, Soding J, Lupas AN.** 2006. The MPI Bioinformatics Toolkit for protein sequence analysis. Nucleic Acids Res. **34:**W335–W339. http://dx.doi.org/10.1093/nar/gkl217.
53. **Dulebohn DP, Bestor A, Rego RO, Stewart PE, Rosa PA.** 2011. *Borrelia burgdorferi* linear plasmid 38 is dispensable for completion of the mouse-tick infectious cycle. Infect. Immun. **79:**3510–3517. http://dx.doi.org/10.1128/IAI.05014-11.
54. **Purser JE, Lawrenz MB, Caimano MJ, Howell JK, Radolf JD, Norris SJ.** 2003. A plasmid-encoded nicotinamidase (PncA) is essential for infectivity of *Borrelia burgdorferi* in a mammalian host. Mol. Microbiol. **48:**753–764. http://dx.doi.org/10.1046/j.1365-2958.2003.03452.x.